Petroleum Science 23 (2026) 3299–3319

Contents lists available at ScienceDirect

Petroleum Science

journal homepage: www.keaipublishing.com/en/journals/petroleum-science

Original Paper

Multi-spherical interactions driving the generation, accumulation and distribution of natural gases and CO_2 resources in the Changling Fault Depression, Songliao Basin, China

Ming-Ming Jiang [a], Si-Shuo Zhou [b], Xin Yan [c], Quan-You Liu [a,*]

[a] Institute of Energy, School of Earth and Space Sciences, Peking University, Beijing, 100871, China
[b] School of Earth Science, Northeast Petroleum University, Daqing, 163318, Heilongjiang, China
[c] Gas Production Branch Company of Daqing Oil Field Company Co., Ltd., PetroChina, Daqing, 163000, Heilongjiang, China

A R T I C L E I N F O

Article history:
Received 16 March 2025
Received in revised form
21 November 2025
Accepted 5 February 2026
Available online 11 February 2026

Edited by Min Li

Keywords:
Songliao Basin
Multi-spherical interaction
CO_2 gas reservoir
Petroleum geology

A B S T R A C T

This study systematically investigates the genesis, migration, accumulation, and distribution patterns of natural gas and CO_2 in the Changling Fault Depression of the Songliao Basin through an interdisciplinary Earth system framework, focusing on multi-sphere interactions. Integrated analyses employing gas geochemistry, numerical simulations, and core observations reveal that deep magmatic-hydrothermal processes (lithosphere) provide the primary heat and fluid sources, paleoclimate oscillations (atmosphere) modulate organic productivity and preservation efficiency, and lacustrine-level fluctuations (hydrosphere) control reservoir connectivity and gas-phase partitioning. These synergistic controls jointly determine hydrocarbon generation in source rocks, volcanic reservoir evolution, and CO_2-CH_4 competitive accumulation. Results indicate that natural gas within the Changling Fault Depression is predominantly thermogenic with localized abiotic contributions, as evidenced by $\delta^{13}C_1$ values ranging from −56.8‰ to −1.7‰ and the coexistence of both normal and reversed carbon isotopic fractionation sequences. CO_2 exhibits a dominant inorganic mantle-derived origin, characterized by $\delta^{13}CO_2$ values between −18.9‰ and −0.6‰. Thermogenic gas preferentially accumulates in volcanic reservoirs of the Quantou and Yingcheng Formations, while CO_2 and CH_4 display planarly complementary distributions, with high-CO_2 concentrations localized in the eastern Changshen area corresponding to low-CH_4 zones. Paleoenvironmental reconstructions reveal a progressive transition from deep to shallow lacustrine conditions, from humid to semi-arid climate regimes, and from freshwater to brackish depositional environments during the Early Cretaceous. Source rocks of the Shahezi Formation exhibit stronger primary productivity and higher hydrocarbon generation potential than those of the Yingcheng Formation, driven by coupled effects of tectonic subsidence, volcanic nutrient input, and redox-controlled organic preservation. Tectonic evolution governs vertical hydrocarbon migration and mantle-derived CO_2 influx through volcanic activity and fault system development, whereas climate-sedimentation coupling under Ferrel circulation and global eustatic cycles regulates organic matter enrichment. This integrated analysis establishes a comprehensive framework for volcanic gas reservoir exploration and CO_2 geological sequestration, contributing to the synergistic advancement of carbon neutrality and energy security strategies.

© 2026 The Authors. Publishing services by Elsevier B.V. on behalf of KeAi Communications Co. Ltd. This is an open access article under the CC BY license (http://creativecommons.org/licenses/by/4.0/).

1. Introduction

The Earth system constitutes a dynamically coupled framework comprising the lithosphere, hydrosphere, atmosphere, and biosphere, whose interactions govern geological evolution and resource distribution through material and energy exchange (Bowring et al., 2022; Jin et al., 2023; Zhang et al., 2024b; Zhu et al., 2024). Recent advances have highlighted the critical role of multi-

* Corresponding author.
E-mail address: liuqy@pku.edu.cn (Q.-Y. Liu).
Peer review under the responsibility of China University of Petroleum (Beijing).

https://doi.org/10.1016/j.petsci.2026.02.006
1995-8226/© 2026 The Authors. Publishing services by Elsevier B.V. on behalf of KeAi Communications Co. Ltd. This is an open access article under the CC BY license (http://creativecommons.org/licenses/by/4.0/).

sphere interactions in controlling hydrocarbon formation and accumulation, emerging as a focal point in international geoscience research (Liu et al., 2019; Zhu et al., 2024). For instance, mantle upwelling driven by plate tectonics triggers volcanic activity that accelerates thermal maturation of source rocks (Van Der Meer et al., 2014; Li et al., 2018), while eustatic cycles and paleoclimatic variations regulate organic matter enrichment and preservation efficiency through depositional environment modulation (Wei et al., 2023; Wang et al., 2024b; Zhang et al., 2024b). Concurrently, thermo-tectonic events dictate hydrocarbon migration pathways and trap formation via lithospheric stress field adjustments (Scotese, 2021; Zhu et al., 2024). Studies demonstrate that petroleum systems fundamentally arise from synergistic deep-to-shallow sphere interactions, requiring multidimensional analysis integrating deep crustal dynamics (Alcott et al., 2024), surface climatic conditions (Zhou et al., 2023), and biological processes (Boscolo-Galazzo et al., 2021) to unravel their spatiotemporal distribution patterns (Inguaggiato et al., 2018; Jiang and Liu, 2025).

The Changling Fault Depression in the Songliao Basin, a strategic hydrocarbon replacement zone in northeastern China, has proven natural gas reserves exceeding 100 billion cubic meters and CO_2 resources on the scale of tens of billions of cubic meters after decades of exploration (Liu et al., 2017a; Liu et al., 2021; Liu et al., 2023a). However, the region exhibits complex same-source heterogeneous storage and multi-source superposition distribution patterns of natural gas and CO_2, with current studies predominantly emphasizing single-sphere controls (e.g., structural frameworks or source rock characteristics), resulting in limited effectiveness in delineating favorable exploration targets (Liu et al., 2016; Lu et al., 2020; Liu et al., 2023a). Exploration practices reveal significant discrepancies in the traditional source-reservoir-seal triad model when predicting spatial distributions of volcanic gas reservoirs and mantle-derived CO_2 accumulations (Fu et al., 2014; Meng et al., 2014; Liu et al., 2018; Liu et al., 2023a), particularly due to inadequate understanding of coupling mechanisms between deep magmatic-fluid systems and shallow sedimentary responses, which constrains prediction accuracy for hydrocarbon enrichment patterns (Jiang et al., 2025b). Furthermore, the competitive charging processes and preservation conditions between CO_2 (as a strategic alternative energy resource and carbon sequestration target) and CH_4 require systematic investigation (Etiope et al., 2011; Brand et al., 2012; Chen et al., 2021; Huang et al., 2021). Consequently, deciphering gas accumulation mechanisms through a multi-sphere interaction framework holds dual significance for enhancing exploration efficiency and supporting carbon neutrality objectives, necessitating integrated analysis of lithospheric deformation dynamics, magmatic-thermal perturbations, and climate-driven depositional cyclicity in reservoir formation studies (Brune et al., 2017; Gao et al., 2017; Hemingway et al., 2018; Rizzo et al., 2018; Zhang et al., 2024a).

Focusing on the Changling Fault Depression, this investigation reexamines the complete generation-migration-accumulation processes of natural gas and CO_2 through an Earth multi-sphere interaction framework, aiming to transcend conventional petroleum geology paradigms and develop novel methodologies for prospective resource prediction. By elucidating the synergistic controls of deep magmatic-hydrothermal processes (lithosphere), paleoclimatic oscillations (atmosphere), and lacustrine level fluctuations (hydrosphere) on hydrocarbon generation in source rocks, volcanic reservoir formation, and gas and CO_2 competitive accumulation, this study establishes a comprehensive multi-parameter coupling model for favorable zone identification and exploration optimization. In addition to traditional gas geochemistry and structural analysis, gas geochemistry, trace-element and TOC-based paleoenvironmental reconstruction were applied. These data provide new quantitative evidence for assessing the coupled influence of redox conditions, paleoclimate variability, and paleoproductivity on source rock quality. Our results demonstrate that strong water column reducing conditions and humid climate regimes are key to the development of high-quality source rocks in the Early Cretaceous, and that volcanic nutrient input and basin evolution jointly modulate organic matter enrichment and preservation efficiency. This systematic approach advances Earth system science by decoding deep-shallow sphere coupling mechanisms in sedimentary basins.

2. Geological setting

The Songliao Basin, the most prolific hydrocarbon-bearing basin in Northeast China (Fig. 1(a)), encompasses approximately 260,000 km^2 with proven large-scale gas accumulations in deep strata (Tang et al., 2017; Liu et al., 2018; Liu et al., 2023a). Structurally classified as a Mesozoic semi-graben continental rift basin, the study area focuses on the Changling Fault Depression situated in the southern sector of the basin (Fig. 1(b)) (Cheng et al., 2020).

During the Meso-Cenozoic, Northeast China entered an intraplate tectonic evolutionary phase following the collision between the Siberian and North China blocks, governed by the evolution of the Circum-Pacific tectonic domain (Zhang et al., 2015; Chen et al., 2017; Liu et al., 2022). The Songliao Basin occupies the northern margin of this domain in eastern Asia (Cheng et al., 2020). In the Eocene (53–35 Ma), termination of the Kula-Pacific spreading ridge initiated northwestward subduction of the Pacific Plate beneath the Eurasian Plate (Chen et al., 2017). Subsequently, since the Oligocene, intensified NW-NWW-trending subduction has driven deep thermal upwelling, facilitating formation of marginal sea basins including the Japan Sea and Okhotsk Basin (Cheng et al., 2020). Concurrently, the intracontinental Songliao Basin experienced NW-NWW-trending compressional stress regimes. The tectonic evolution demonstrates progressive stress regime transitions: Late Jurassic-Early Cretaceous NNW-NNE-trending sinistral transtension, Mid-Late Early Cretaceous-Paleocene NW-trending compression, Eocene NE-NEE-trending weak extension, and NW-NWW-trending compression since the Oligocene (Cheng et al., 2020).

The basement comprises pre-Paleozoic and Paleozoic metamorphic and volcanic rocks formed during the Hercynian orogeny, capped by a regional weathering unconformity (Huang et al., 2004; Liu et al., 2018). The rift structural layer consists of Upper Jurassic Huoshiling Formation (J_3h) and Lower Cretaceous Shahezi (K_1sh), Yingcheng (K_1yc), and Denglouku (K_1d) Formations (Fig. 2) (Liu et al., 2018). The depression structural layer includes Lower Cretaceous Quantou (K_1q), Middle Cretaceous Qingshankou (K_2qs), Yaojia (K_2y), and Nenjiang (K_2n) Formations, while the inversion structural layer comprises Middle Cretaceous Sifangtai (K_2s) and Mingshui (K_2m) Formations (Liu et al., 2018). This stratigraphic architecture records multiple phases of tectonic reorganization, initially dominated by NNE-trending normal faulting during rift development, subsequently transitioning to NW-trending thrust systems during basin inversion stages (Fu et al., 2010, 2023; Liu et al., 2023a).

3. Materials and methods

3.1. Data sources

This study integrates both newly acquired experimental data and published regional datasets. Gas geochemical data were obtained from 28 wells in the Changling Fault Depression through direct sampling and analysis, while regional geochemistry data were compiled from previously published studies and exploration reports (Li et al., 2017). To reduce this source of bias and preserve the geological fidelity of gas origin analysis, only samples collected

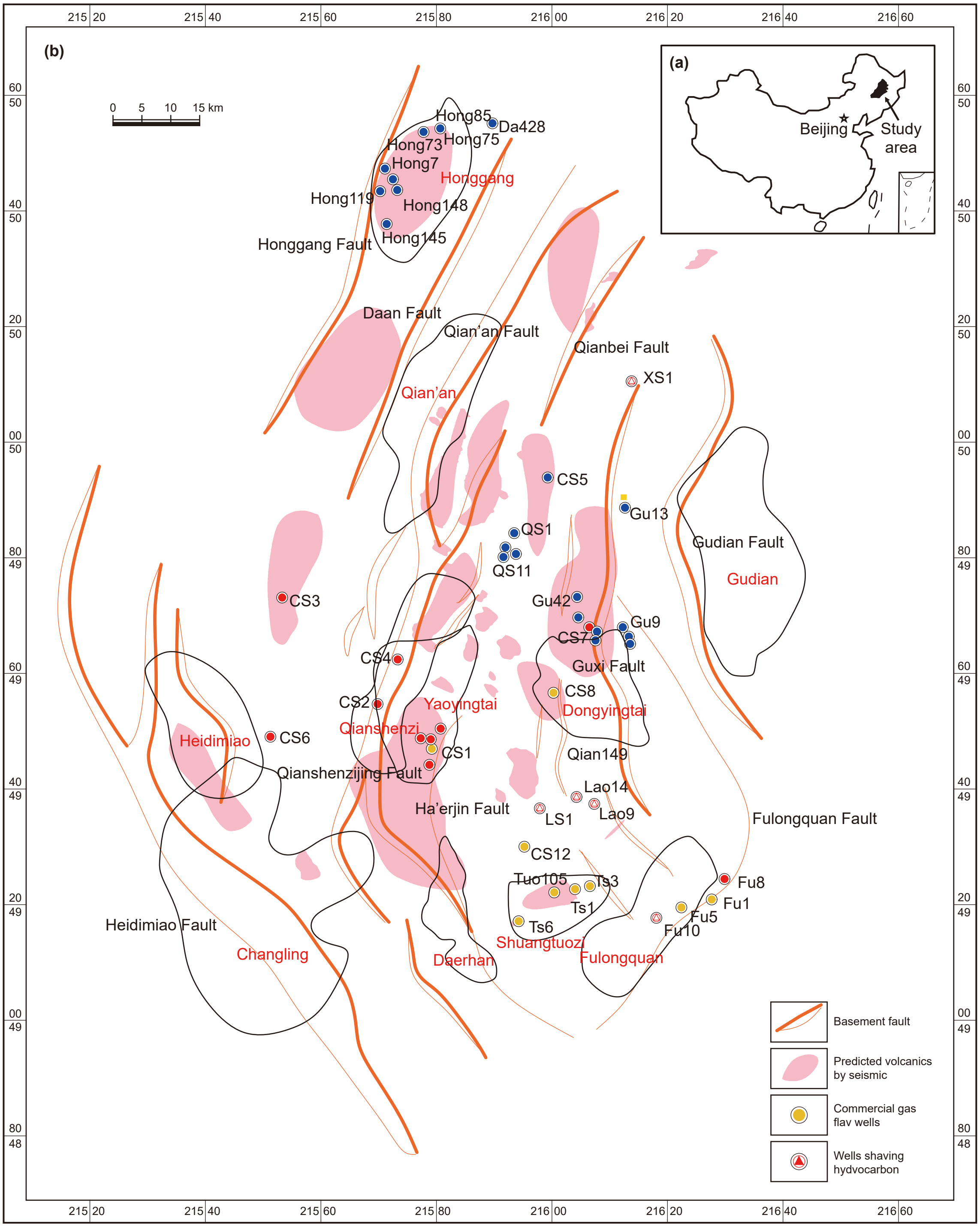

Fig. 1. Geological setting of the Songliao Basin. **(a)** Geographical location of the Songliao Basin in China; **(b)** Distribution of volcanic rocks and basement faults in the Changling Fault Depression, Songliao Basin.

within the first five years of production were prioritized in this study, as they are more likely to represent the pre-disturbance equilibrium conditions of the reservoir. This approach ensures higher confidence in the interpretation of relative gas abundance, origins and others.

3.2. Experimental analyses

New gas samples collected from the 28 wells were obtained using stainless-steel cylinders. Molecular compositions were determined using an HP 5890-II gas chromatograph, and alkane gas components and carbon isotopes ($\delta^{13}C$) were analyzed using a Finnigan MAT-252 mass spectrometer. Raman spectroscopic analysis of fluid inclusions was performed to constrain paleo-fluid composition and thermal evolution. Mudstone samples from the Huoshiling, Shahezi, and Yingcheng Formations were analyzed for metal element concentrations via Vista MPX ICP-OES, and total organic carbon (TOC) was measured using a CS-200 analyzer. Thin-section observations and logging curve analyses (e.g., Well YS1)

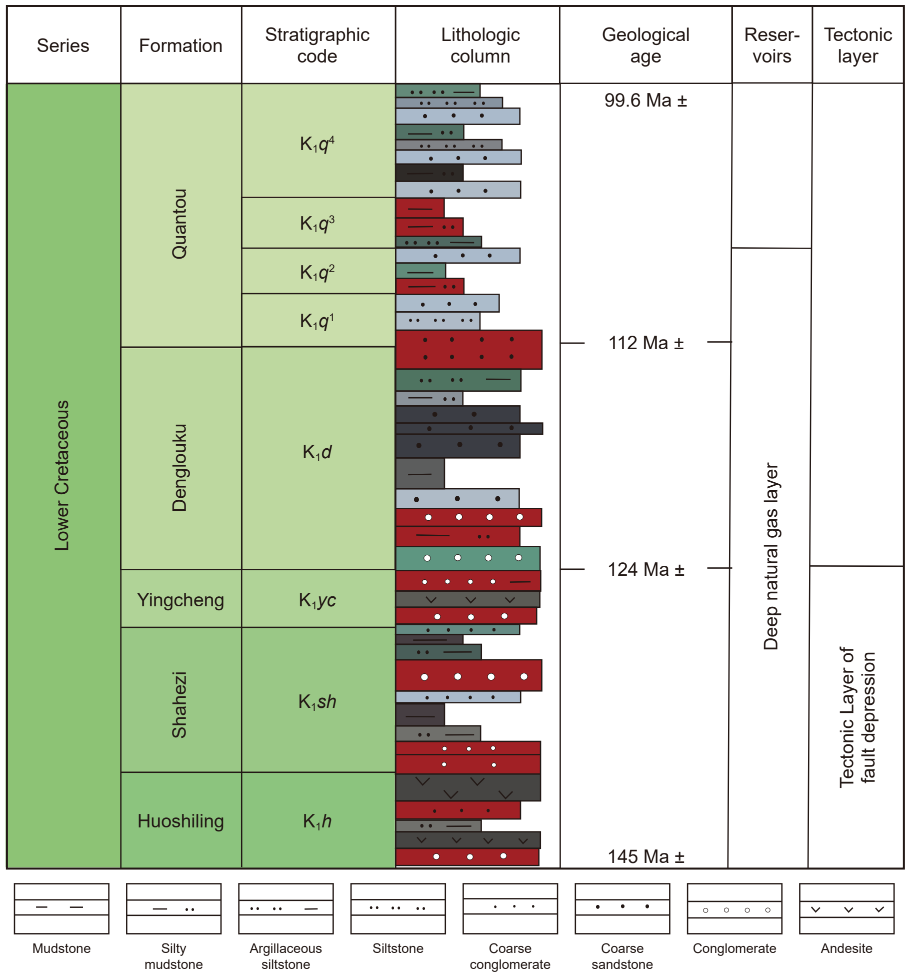

Fig. 2. Stratigraphic column of the Changling Fault Depression, Songliao Basin. The colors of series, formations, and stratigraphic codes are consistent with international stratigraphic color standards.

were used to characterize pore-throat structures, mineral assemblages, and reservoir-caprock configurations. All depths reported refer to average sampling depths within the corresponding stratigraphic units.

3.3. Numerical and comparative analysis

To interpret compositional patterns, vertical and planar gas distributions were simulated using an in-house numerical code incorporating migration-diffusion coupling mechanisms. Comparative isotopic analyses ($\delta^{13}C_1$-$\delta^{13}C_{CO_2}$, $\delta^{13}C_1$-$\delta^{13}C_2$-$\delta^{13}C_3$) were used to distinguish thermogenic, biogenic, and abiogenic gas sources. These results were integrated with previously published gas geochemical datasets to validate model outputs and regionalize gas accumulation mechanisms.

3.4. Analytical framework

This multi-proxy analytical framework—combining direct geochemical, petrographic, and isotopic evidence with regional synthesis—enables a systematic evaluation of genetic linkages between mantle-derived CO_2 plumes and hydrocarbon accumulations in complex volcanic reservoirs.

4. Results

4.1. Geochemical characteristics of natural gases and CO_2

4.1.1. Compositional characteristics of natural gases

CH_4 in the Changling Fault Depression exhibits depth-dependent enrichment patterns, with high-concentration zones clustered between 1800 and 2370 m and 3214–4040 m (Fig. 3(a)). Elevated CH_4 concentrations (60%–97.43%) are predominantly observed in the Gudian, Changshen, and Changling areas, particularly within the 3500 m–3600 m interval. Moderate CH_4 concentrations (60%–80%) occur in the Changshen, Yaoyingtai, and Daerhan areas. Shallower intervals (0 m–2370 m) are dominated by lower CH_4 concentrations (0%–25%), primarily in the Qian'an and Honggang areas. Notably, distinct low-CH_4 zones (<25%) are localized in the Changshen area (3560–3900 m) and Qian'an and Honggang areas (1900–2270 m).

Higher molecular-weight hydrocarbons (C_2H_6, C_3H_8, C_4H_{10}) are preferentially enriched at 3500–4040 m (Fig. 3(b)–(d)). Elevated C_2H_6 concentrations (up to 12.5%) and higher alkane contents (>2%) dominate the Changling, Qian'an, and Honggang areas at 1890–2550 m. In contrast, lower alkane concentrations (<2%) characterize the Changshen, Changling, and Gudian areas at 1200–2270 m.

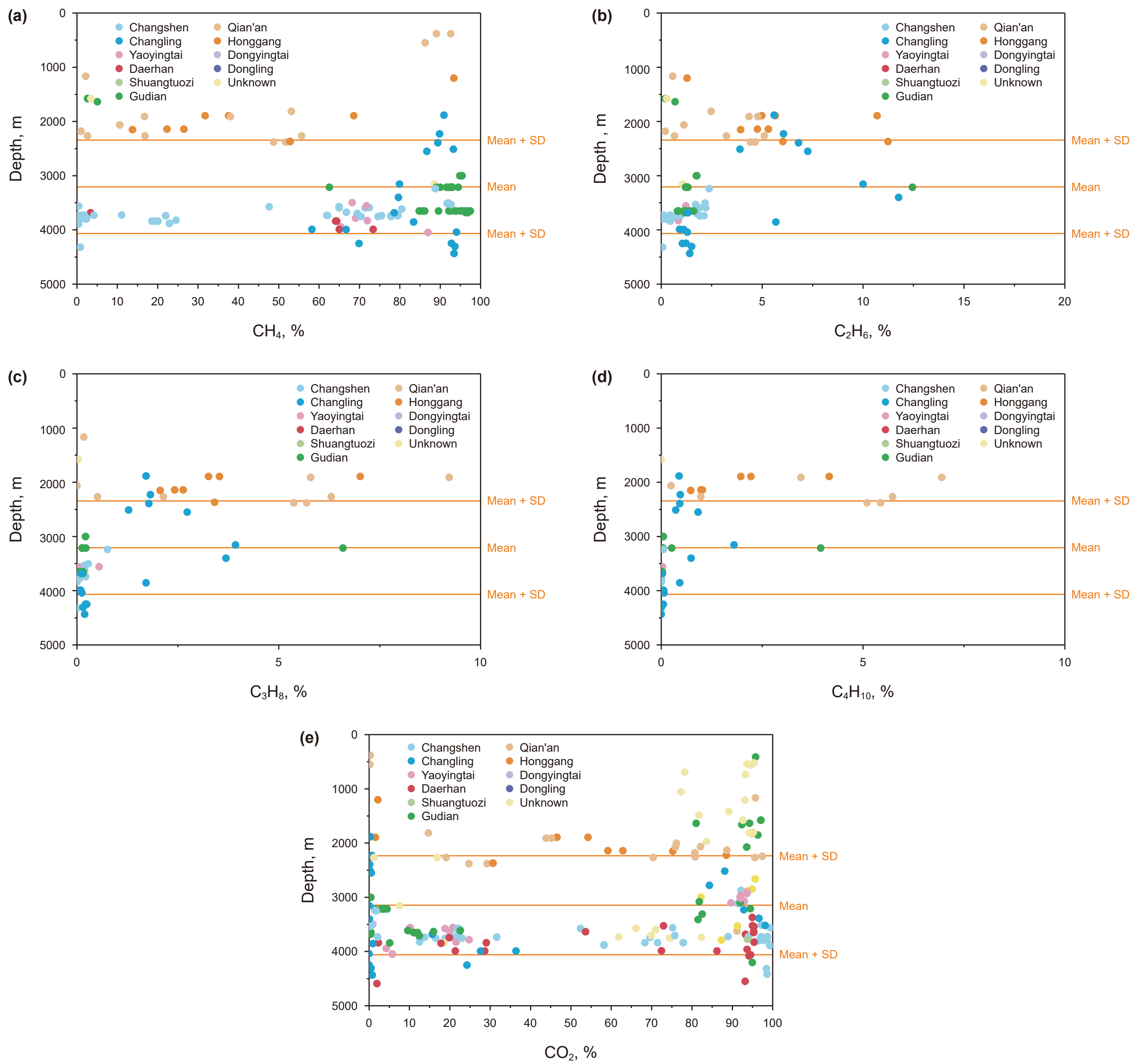

Fig. 3. Variation of natural gases components with depth in the Changling Fault Depression, Songliao Basin. Natural gas components: **(a)** CH_4, **(b)** C_2H_6, **(c)** C_3H_8, **(d)** C_4H_{10}, and **(e)** CO_2.

4.1.2. Carbon isotopic characteristics of natural gases

$\delta^{13}C_1$ display significant depth-dependent variability (Fig. 4(a)). In deeper intervals (3000–4130 m), $\delta^{13}C_1$ values range from −30‰ to −16.54‰, corresponding to the Changshen, Yaoyingtai, Daerhan, and Gudian regions. Shallower depths (380–2540 m) exhibit bimodal isotopic trends: a narrow range (−11.9‰ to −1.7‰) in the Changling area and a broader distribution (−56.8‰ to −23.2‰) in Qian'an, Honggang, and Dongling areas. Carbon isotopic sequences show both normal ($\delta^{13}C_1 < \delta^{13}C_2 < \delta^{13}C_3$) and reversed patterns (Fig. 4(c)), including partial reversals ($\delta^{13}C_1 > \delta^{13}C_2$ or $\delta^{13}C_2 > \delta^{13}C_3$) and complete reversals ($\delta^{13}C_1 > \delta^{13}C_2 > \delta^{13}C_3$). These anomalies likely reflect mixing of thermogenic and abiogenic gas sources.

4.1.3. Compositional characteristics of CO_2

CO_2 in the Changling Fault Depression displays bimodal enrichment zones at 400–2550 m and 2850–4550 m, exhibiting significant concentration differentiation (Fig. 3(e)). High CO_2 concentrations (50%–99.45%) dominate across multiple regions, with ultrahigh values (>80%) predominantly occurring at 2660–4550 m. Moderate-high CO_2 contents (60%–80%) are concentrated in the Changshen and Daerhan areas at 3520–4000 m, while similar ranges are observed in Qian'an and Honggang areas at shallower depths (2000–2270 m). Low-to-moderate CO_2 concentrations (0%–30%) are widely distributed, with intermediate values (10%–30%) prevalent at 3550–4000 m. Notably, low CO_2 concentrations (<10%) are localized in the Changshen, Changling, Daerhan, and Gudian areas at 3000–4590 m, as well as in the Changling and Honggang areas at 1890–2550 m.

4.1.4. Carbon isotopic characteristics of CO_2

The $\delta^{13}C_{CO_2}$ values range from −18.9‰ to −0.6‰, with the majority of samples clustered between 3470 and 4050 m (Fig. 4(b)). These isotopic characteristics are primarily associated with the Changling, Yaoyingtai, Qian'an, and Gudian areas. The narrow isotopic range and positive $\delta^{13}C_{CO_2}$ values (>−8‰) in

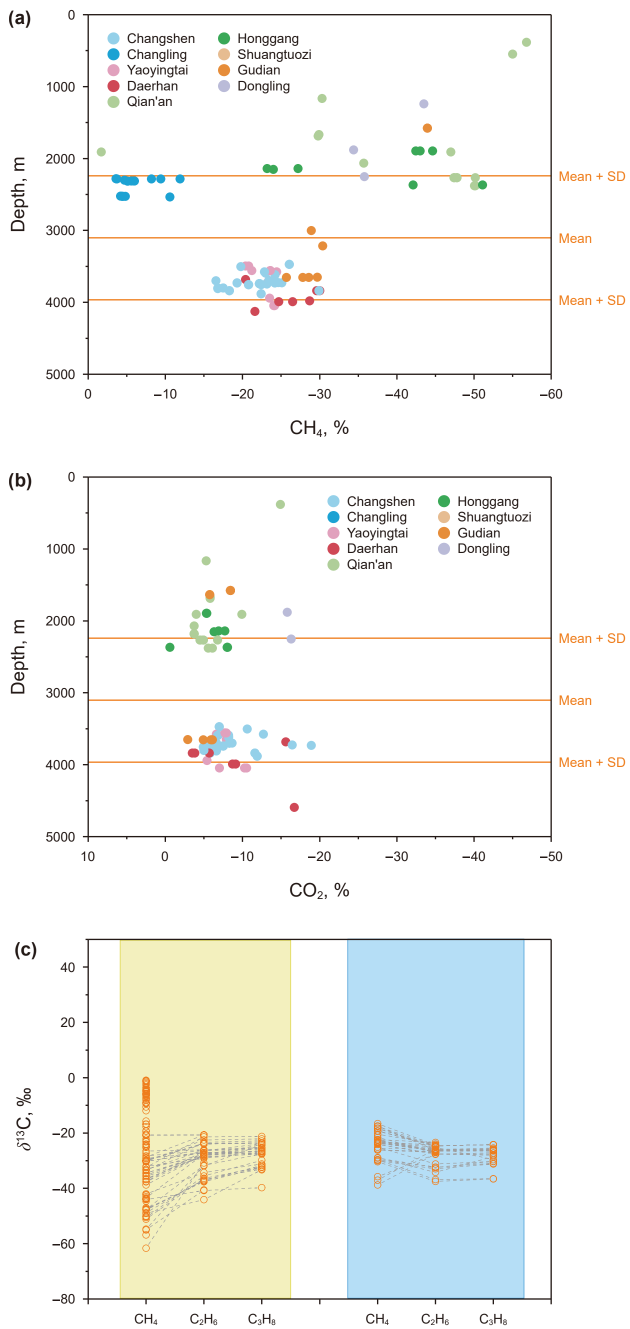

Fig. 4. Variation of carbon isotopes in natural gases with depth in the Changling Fault Depression, Songliao Basin. Carbon isotopes: **(a)** δ^{13}C-CH_4, and **(b)** δ^{13}C-CO_2. **(c)** Relationships among δ^{13}C-CH_4, δ^{13}C-C_2H_6 and δ^{13}C-C_3H_8.

deeper intervals (3800–4200 m) suggest a predominant mantle-derived origin, while lighter values (−18.9‰ to −10‰) at shallower depths (2200–3200 m) may reflect mixing with organically derived CO_2 or isotopic fractionation during migration. This vertical isotopic stratification correlates with magmatic degassing intensity and fault-controlled fluid pathways, further supporting the hypothesis of multi-source CO_2 contributions modulated by lithospheric architecture.

Trace gases (N_2, H_2, He) are discussed in Supplementary Materials, with brief summary provided here: He enrichments co-locate with deep faults, supporting deep-fluid pathways for mantle-derived CO_2. N_2 shows bimodal depth distribution suggesting mixed crustal and atmospheric or organic sources. H_2 occurs at trace levels and may indicate limited abiotic contributions.

4.2. Distribution of natural gases and CO_2 resources

4.2.1. Vertical distribution of natural gases

CH_4 and higher hydrocarbons (C_2H_6, C_3H_8, C_4H_{10}) exhibit distinct stratigraphic partitioning within the Quantou, Denglouku, Yingcheng, Huoshiling Formations, and basement strata (Fig. 5(a)–(d)). Ultrahigh CH_4 concentrations (>80%) are predominantly concentrated in the Quantou Formation of Dongling, Denglouku Formation of Changling, and Huoshiling Formation of Gudian, with minor occurrences in the Yingcheng Formation of Qian'an (Fig. 5(a)). Elevated CH_4 levels (60%–80%) dominate the Yingcheng Formation across the Changshen, Yaoyingtai, and Daerhan regions, while reduced CH_4 concentrations (<20%) characterize the Quantou Formation in Qian'an and Yingcheng Formation in Changshen.

C_2H_6 enrichment (>10%) is localized in the Yingcheng Formation of Changling and Quantou Formation of Honggang (Fig. 5(b)), whereas lower C_2H_6 contents (<10%) occur in the Denglouku and Yingcheng Formations of Changling, along with the Huoshiling Formation in Shuangtaizi and Gudian. Elevated C_3H_8, and C_4H_{10} concentrations (>1%) are preferentially distributed in the Denglouku and Yingcheng Formations of Changling, as well as the Quantou Formation of Honggang (Fig. 5(c) and (d)).

4.2.2. Planar distribution of natural gases

Planarly, high-CH_4 zones dominate the central and western sectors of the Changling Fault Depression, contrasting with lower concentrations in the eastern Changshen and Daerhan areas (Fig. 6(a)). Elevated C_2H_6 accumulations are restricted to the northern portion of the depression, while reduced values prevail in the eastern Changshen and Yaoyingtai regions (Fig. 6(b)). This planar heterogeneity reflects differential hydrocarbon migration pathways controlled by fault-anticline architectures and reservoir quality variations, where central uplift zones favor gas retention while eastern slope belts experience greater leakage through permeable carrier beds.

4.2.3. Vertical distribution of CO_2

CO_2 exhibits a stratigraphic distribution pattern inversely correlated with methane CH_4, where high-CH_4 zones typically correspond to low-CO_2 intervals. CO_2 enrichment occurs primarily within the Quantou, Yingcheng, Huoshiling Formations, and basement strata (Fig. 5(e)). Ultrahigh CO_2 concentrations (>80%) are localized in the Quantou Formation of Qian'an, Gudian, and Donggang, the Yingcheng Formation of Changshen and Daerhan, with minor occurrences in the Denglouku Formation of Changshen. Elevated CO_2 levels (60%–80%) dominate the Quantou Formation in Qian'an and Yingcheng Formation in Changshen, while low-CO_2 zones (<20%) characterize the Yingcheng Formation across multiple areas, the Huoshiling Formation in Guadian, and basement units in Honggang area.

4.2.4. Planar distribution of CO_2

Planarly, CO_2-rich areas exhibit a complementary relationship with CH_4 accumulations, particularly evident in the eastern Changshen and Yaoyingtai regions where low-CH_4 zones coincide with high-CO_2 concentrations (Fig. 6(c)). This inverse distribution highlights competitive charging mechanisms between hydrocarbon and mantle-derived CO_2 systems, where fault-controlled conduits preferentially channel deep-sourced CO_2 into structural traps that overlap or displace pre-existing gas accumulations. The planar segregation further underscores the role of differential migration efficiency and reservoir-caprock integrity in governing fluid phase distribution.

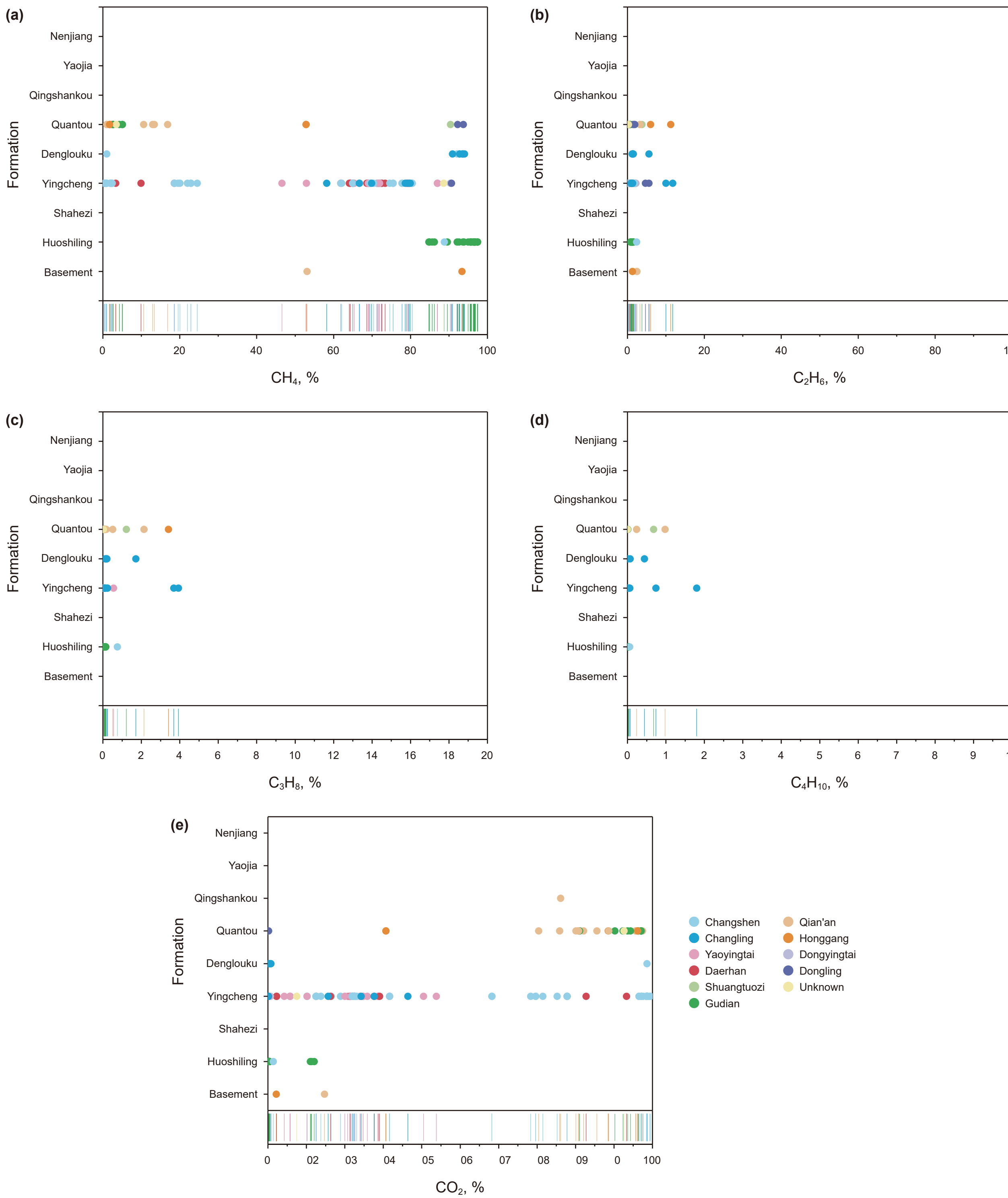

Fig. 5. Vertical distribution of natural gas components and concentrations across different stratigraphic units in the Changling Fault Depression, Songliao Basin. Natural gas components: **(a)** CH_4, **(b)** C_2H_6, **(c)** C_3H_8, **(d)** C_4H_{10}, and **(e)** CO_2.

4.3. Generation and accumulation of natural gases and CO_2 resources

4.3.1. Generation and accumulation of natural gases

Carbon isotopic compositions ($\delta^{13}C_1$ and $\delta^{13}C_{CO_2}$) indicate mixed thermogenic and abiogenic origins for methane in the Changling Fault Depression. Thermogenic gas, predominantly late-mature oil-cracked gas, dominates in the Changshen, Yaoyingtai, and Gudian areas, as evidenced by $\delta^{13}C_1$ values (−35‰ to −28‰) and C_2+ homolog distributions (Fig. 7(a)–(c)). The Qian'an area exhibits dual-sourced methane, combining thermogenic ($\delta^{13}C_1$: −32‰ to −25‰) and abiogenic components ($\delta^{13}C_1$: −18‰ to −12‰), with the latter potentially linked to mantle-derived fluids or Fischer-Tropsch synthesis. $\delta^{13}C_2$ and $\delta^{13}C_3$ data further

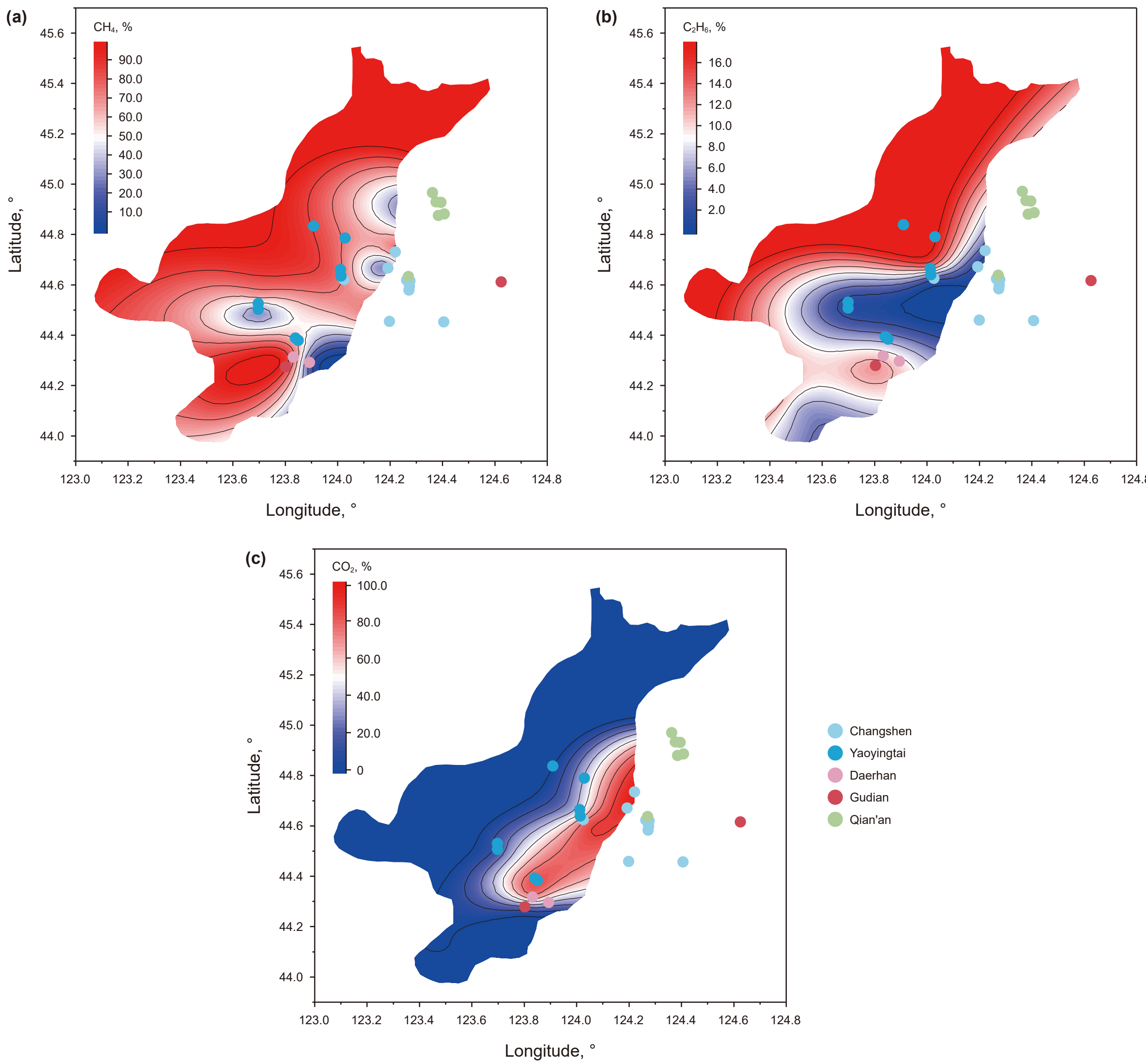

Fig. 6. Planar distribution of natural gas components and concentrations across well locations in the Yingcheng Formation of the Changling Fault Depression, Songliao Basin. Natural gas components: **(a)** CH_4, **(b)** C_2H_6, and **(c)** CO_2. Noted, the figure is based on relative volumetric measurements, which reflect the relative abundance of CH_4 and CO_2 rather than their absolute in-place reserves.

reveal minor coal-type gas contributions in Changshen and Daerhan, though isotopic reversals ($\delta^{13}C_1 > \delta^{13}C_2 > \delta^{13}C_3$) and deviations from conventional genetic diagrams suggest abiogenic dominance across most regions. The observed complete isotopic reversals in some samples are likely caused by the superposition of several processes, including the mixing of abiogenic and thermogenic gases. These mechanisms disrupt the conventional isotopic ordering of hydrocarbon chains. Supporting this interpretation, the Bernard plot analysis further confirms a thermogenic origin for most gases in the basin, particularly in the Changshen area where gas samples plot predominantly in Type III thermogenic fields, consistent with an over-mature gas generation stage (Fig. 7(e)). Together, these lines of evidence suggest that isotopic anomalies are not random noise but are geochemically meaningful indicators of complex gas evolution pathways in a structurally heterogeneous volcanic reservoir system.

Gas accumulation mechanisms are classified into near-source and distal-source migration-accumulation systems. Near-source systems involve Shahezi Formation source rocks expelling hydrocarbons through major fault systems into adjacent volcanic reservoirs within the Shahezi or Yingcheng Formations. Vertical migration along fault zones facilitates rapid charging of proximal traps, exemplified by the Gudian gas field. Distal systems, typified by the Yaoyingtai Yingcheng volcanic reservoirs, require complex lateral migration through composite carrier beds (e.g., unconformities, fractured volcanics), with accumulation efficiency governed by caprock integrity and hydrodynamic conditions. The coexistence of these mechanisms reflects tectonic-stage-dependent hydrocarbon redistribution, where early rift-phase faults controlled near-source charging, while later inversion structures enabled long-distance migration through reactivated fracture networks.

4.3.2. Generation and accumulation of CO_2

CO_2 in the Changling Fault Depression is predominantly of inorganic origin, derived from mantle-derived fluids ascending

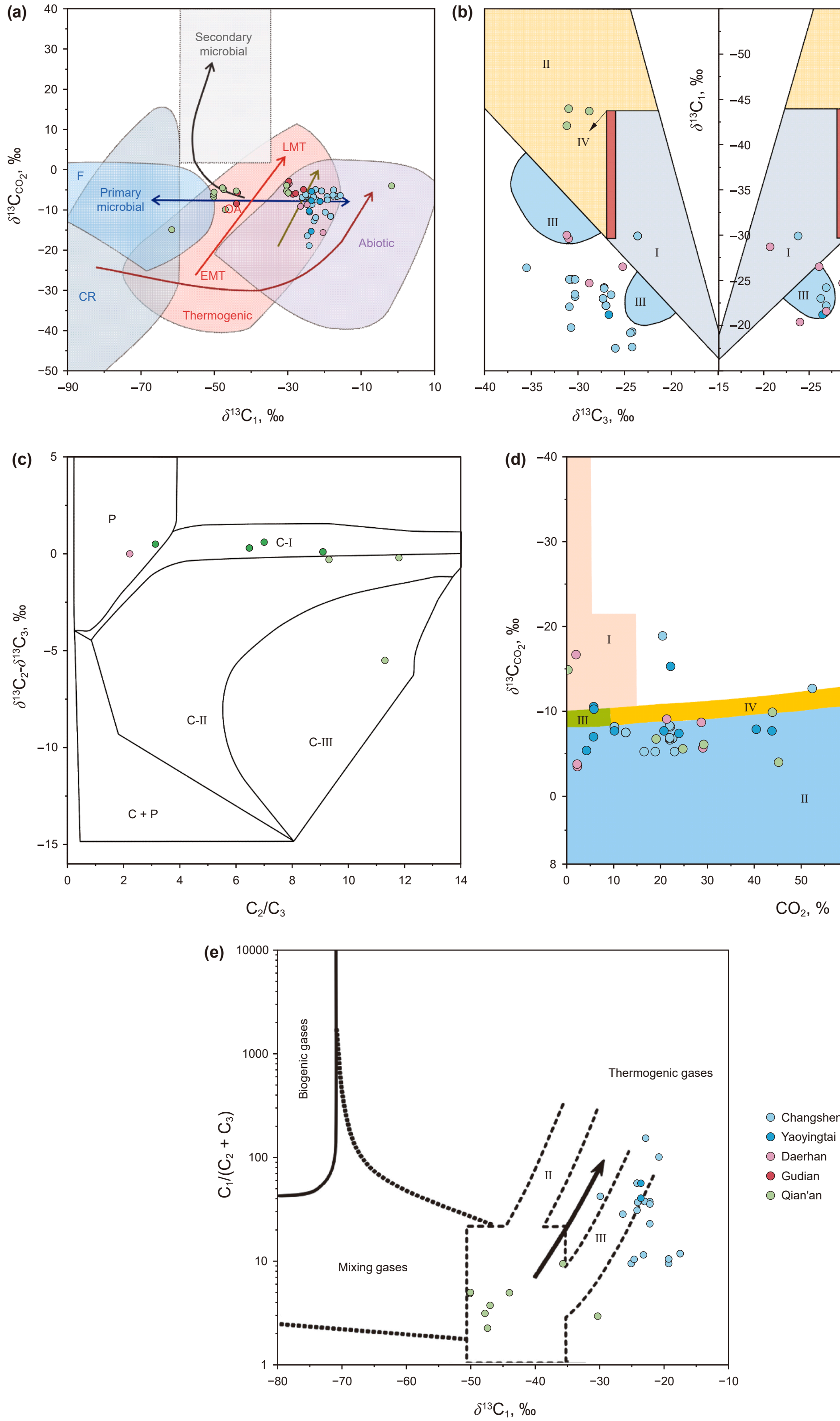

Fig. 7. Origins of CH_4 and CO_2 gases in the Changling Fault Depression. **(a)** Relationship between $\delta^{13}C_1$ and $\delta^{13}C_{CO_2}$, modified from Milkov and Etiope (2018). Abbreviations: CR, carbon dioxide reduction; F, fermentation; EMT, early mature thermogenic gas; OA, oil-associated thermogenic gas; LMT, late mature thermogenic gas; **(b)** Gas type identification based on $\delta^{13}C_1$-$\delta^{13}C_2$-$\delta^{13}C_3$, modified from Dai et al. (2014). Zones: I, coal-derived gas; II, oil-type gas; III, reversal carbon isotopes of mixed gas; IV, coal-derived or oil-type gas; **(c)** Gas type identification based on cracking processes, modified from Lorant et al. (1998). Zones: P, kerogen cracking gas; C-I, oil cracking gas; C-II, condensate oil cracking gas; C-III, cracking gas; C + P, mixture of kerogen cracking gas and oil cracking gas; **(d)** Genetic identification of CO_2 sources, modified from Dai (1992). Zones: I, organic CO_2; II, inorganic CO_2; III, coexistence of organic and inorganic CO_2; IV, mixed organic and inorganic CO_2; **(e)** Natural gas type identification base on $\delta^{13}C_1$ and the $C_1/(C_2 + C_3)$ ratio, modified from Bernard et al. (1978).

through deep-seated faults into reservoirs (Fig. 8). High-concentration inorganic CO_2 dominates the Changshen and Qian'an regions (Fig. 7(d)), while minor organic contributions from organic matter thermal degradation are observed in Daerhan and Qian'an areas. Mixed organic-inorganic CO_2 signatures occur in Yaoyingtai and Changshen areas, reflecting interactions between biogenic carbon recycling and mantle inputs.

The accumulation of CO_2 reservoirs is primarily attributed to: (1) mantle-derived magma underplating and crustal remelting, generating CO_2-rich hybrid magmas; (2) basement fault reactivation driving multi-phase volcanic eruptions (Fig. 8), where early syn-rift volcanics formed reservoir-seal assemblages, while late-stage eruptions injected CO_2 into pre-existing volcanic conduits, with microporosity and fracture networks in volcaniclastics enhancing storage capacity (Fig. 9); (3) post-Yingcheng cessation of basement fault activity, enabling preservation of CO_2 within self-sourced volcanic reservoirs. Notably, the Qianshenzi Fault as a syn-depositional structure controlling fissure-type eruptions dictates reservoir distribution by regulating volcanic vent geometry and fracture permeability (Fig. 8). This fault-mediated accumulation mechanism highlights the critical role of tectono-magmatic coupling in creating spatially constrained, high-purity CO_2 reservoirs with exceptional seal integrity. The coexistence of magmatic degassing pulses and fault-sealing episodes establishes favorable conditions for long-term carbon sequestration in volcanic systems.

5. Discussion

5.1. Influence of tectonic evolution

The Songliao Basin initiated its tectonic evolution during the Jurassic, progressing through four distinct phases that differentially influenced volcanic reservoir development and CO_2 charging (Figs. 10 and 11).

The volcanic reservoir formation stage comprised: (1) Huoshiling-Yingcheng rift phase (192–110 Ma), characterized by high-angle normal faulting under rapid Pacific Plate subduction, which induced asthenospheric upwelling and crustal extension (Chen et al., 2017; Cheng et al., 2020; Lou et al., 2022). This phase generated mafic volcanics during the Huoshiling stage and bimodal (mafic-felsic) volcanic suites during the Yingcheng stage, with peak volcanism occurring at 130–110 Ma (Cheng et al., 2020). (2) Denglouku-Nenjiang sag phase (110–80 Ma), marked by reduced volcanic activity as Pacific subduction decelerated, culminating in maximum lake transgression during the Nenjiang stage with deposition of kilometer-thick lacustrine mudstones and multiple hydrocarbon source beds (Jia et al., 2013; Zhang et al., 2013; Cheng et al., 2020; Liu et al., 2023b).

CO_2 charging occurred during: (1) Sifangtai-Paleocene uplift phase (80–50 Ma, Fig. 10(a)), featuring intensified mafic magmatism with widespread dolerite dikes and basaltic eruptions under persistent extensional regimes (Cao et al., 2018; Cheng et al., 2020). (2) Oligocene-Miocene inversion phase (40–10 Ma, Fig. 10(b)), dominated by NE-trending folding, thrust faulting, and structural modification of strata from Huoshiling to Mingshui stages (Huang et al., 2004; Cheng et al., 2020). This phase coincided with a Pacific Plate subduction direction shift from NNW to NWW and subduction angle reduction from steep to shallow.

Throughout these phases, the Changling Fault Depression experienced NNW-SSE compression, with stress dissipation concentrated along southeastern uplift zones and intra-basinal basement faults, diminishing northwestward (Fig. 8) (Ming et al., 2009; Dong et al., 2014). Structural inversion effects exhibited vertical stratification, influencing progressively shallower strata

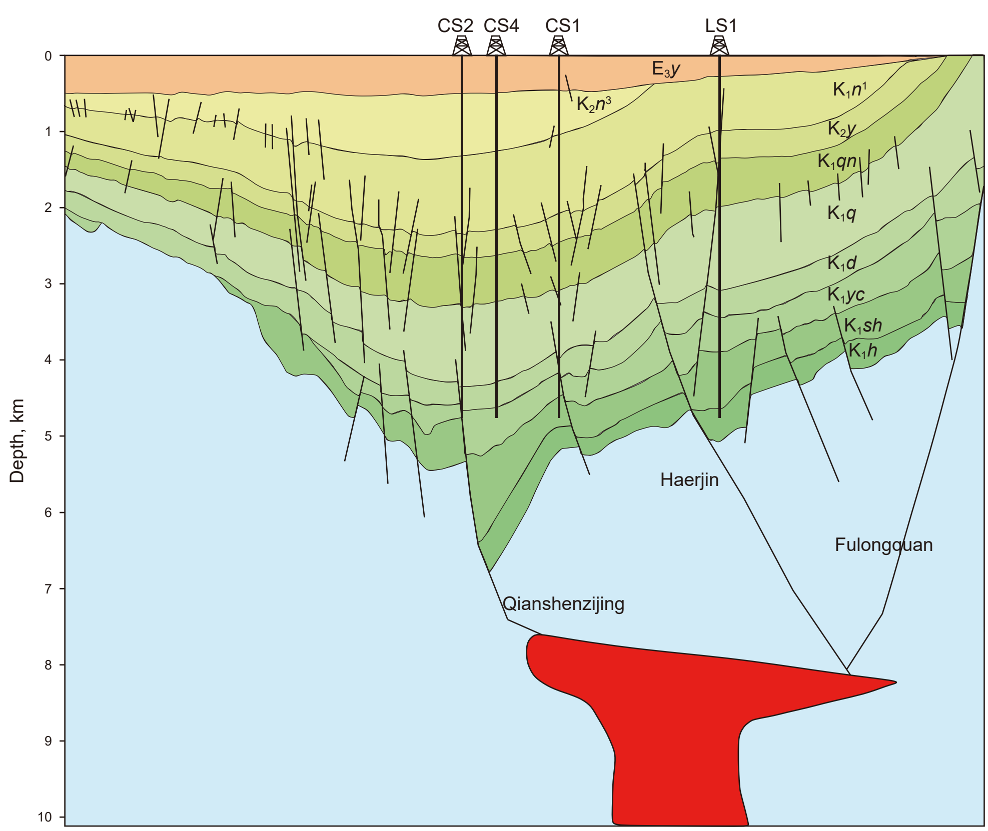

Fig. 8. The stratigraphic profile of mantle fluids intrusion along deep faults in the Changling Fault Depression, Songliao Basin.

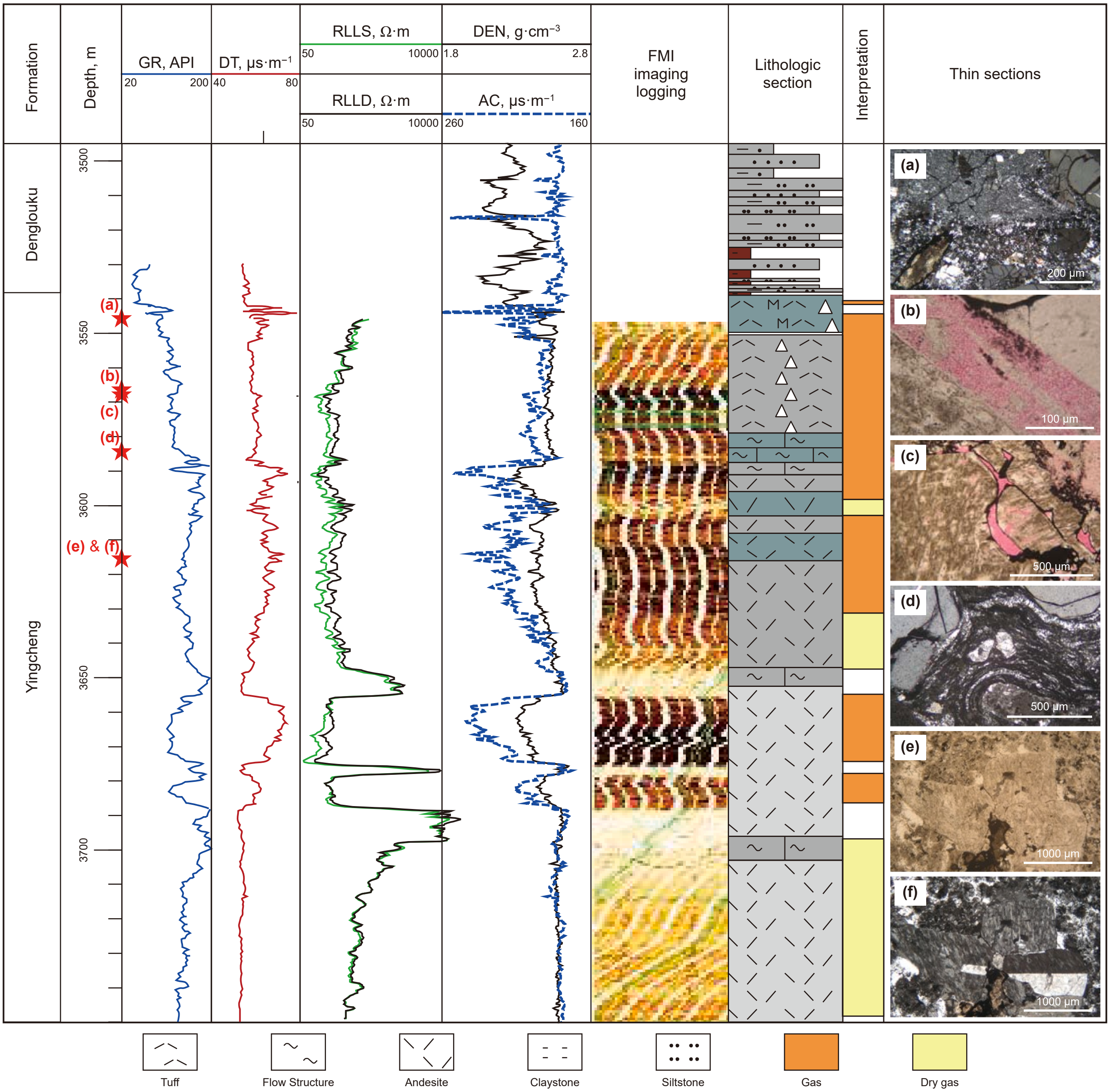

Fig. 9. Well logging curves, lithology, and core thin-section photomicrographs of Well YS1. **(a)** Tuff, 3546 m; **(b)** Tuff breccia, 3567.2 m; **(c)** Tuff breccia, 3568.2 m; **(d)** Flow structures in volcanic rocks, 3584 m; **(e)** Andesite, 3615 m; **(f)** Andesite, 3615 m.

from southeast to northwest. The Oligocene-Miocene inversion ultimately established the current reservoir distribution patterns, where compressional anticlines and fault-sealed traps govern hydrocarbon accumulation, while CO_2 reservoirs are preferentially localized along reactivated volcanic conduits and fracture networks. This spatiotemporal coupling between tectonic reorganization and magmatic-tectonic cycles created vertically stacked, laterally partitioned fluid systems-shallow biogenic methane reservoirs overlying deep thermogenic-abiotic hybrid systems with mantle-derived CO_2 plumes.

Additionally, tectonic evolution exerts a coupled control on the charging and distribution of CH_4 and other non-hydrocarbon gases. Reactivated basement faults and fracture networks not only provided conduits for mantle-derived CO_2 but also governed vertical migration of thermogenic methane expelled from Shahezi Formation source rocks (see vertical/plannar CH_4-CO_2 complementarity in Fig. 6 and migration pathways in Fig. 7). Noblegas signatures (He) and depth-stratified N_2 distributions further indicate that faults act as selective conduits: deep, high-connectivity faults favor ascent of mantle-sourced volatiles (CO_2, He), while low-permeability or laterally extensive carrier beds permit lateral CH_4 migration and trap accumulation. Therefore, as supported by the planar maps in Fig. 6, noble gas and N_2 depth profiles, and the discussion in Section 6, a coupled tectonic-migration model is needed to account for (a) upward advective flux of deep volatiles during magmatic/tectonic pulses, and (b)

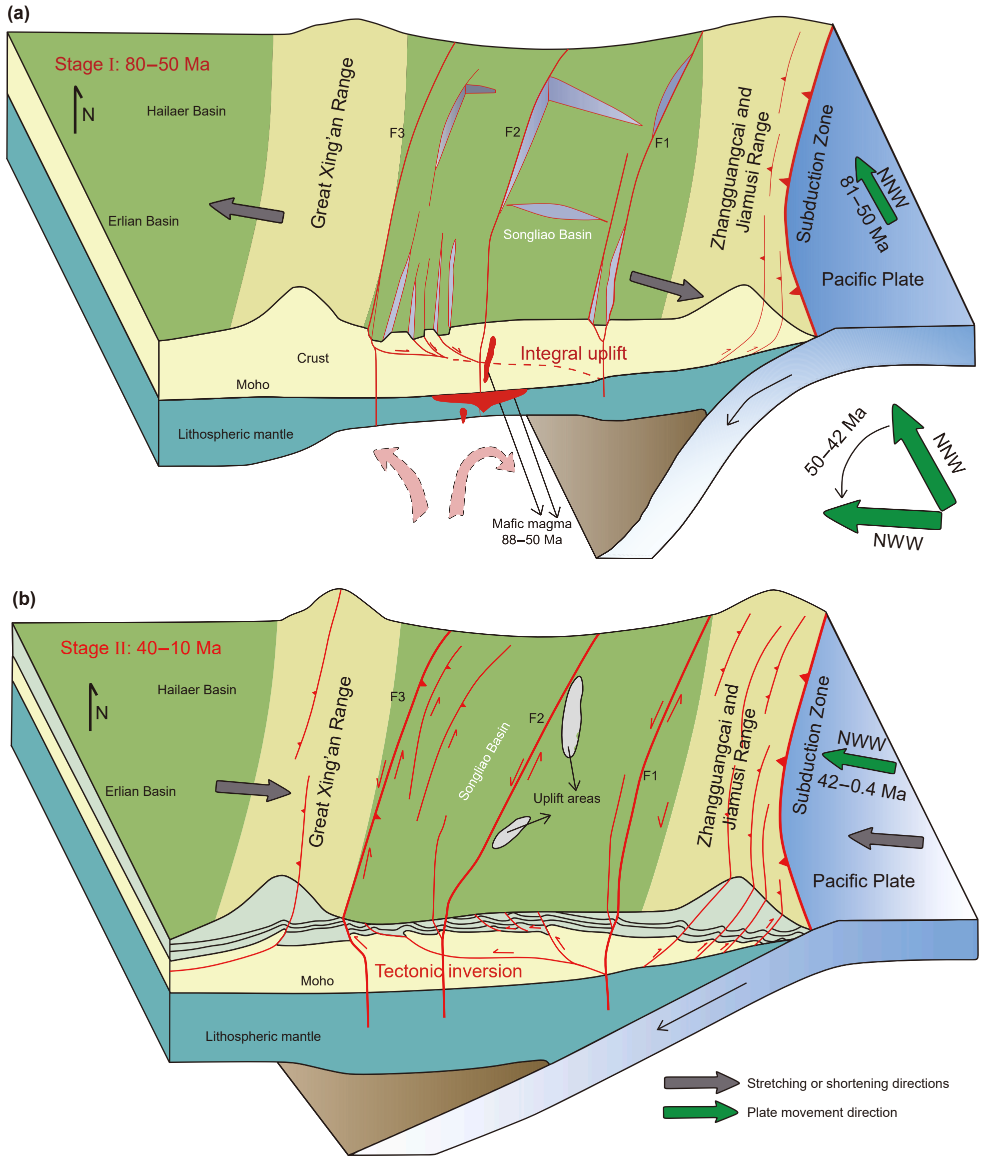

Fig. 10. Three-dimensional model of the tectonic-thermal evolution stages of the Songliao Basin after the Late Cretaceous, modified from Cheng et al. (2020). **(a)** Stage I: Late Cretaceous–Early Paleogene (~80–50 Ma). **(b)** Stage II: Oligocene–Miocene (~40–10 Ma).

simultaneous lateral redistribution of thermogenic CH_4 controlled by carrier-bed architecture and caprock integrity.

It is worth noting that numerous sub-seismic faults were generated during the tectonic evolution of the basin. Although their influence is not the primary focus of this study, it does not imply they are insignificant; on the contrary, they are likely key factors controlling hydrocarbon preservation and migration (Jiang et al., 2023, 2024, 2025a, 2026).

5.2. Influence of climatic evolution

The formation is intrinsically linked to Early Cretaceous rift events, with its unique petroleum system development strongly influenced by mid-latitude Ferrel circulation-driven climatic controls (Figs. 11 and 12). Investigations demonstrate that the Ferrel circulation belt not only played a pivotal role in global polar ice-melt dynamics (Zhu et al., 2024) but also regulated precipitation patterns between 40° and 60°N/S latitudes, fostering organic carbon enrichment in temperate humid zones. This climatic regime, coupled with Cretaceous global oceanic anoxic events (OAEs: OAE1a, OAE1b, OAE2, OAE3) (Barclay et al., 2010; Jenkyns, 2010), jointly facilitated the development of premium source rocks through by enhancing terrestrial nutrient influx and lacustrine primary productivity under Ferrel circulation-induced humid climates, improving organic carbon burial efficiency via water column stratification during OAEs (McArthur et al., 2020), and spatiotemporal coupling of these factors that maintained optimal organic matter production-preservation conditions from mid-Albian to early Late Cretaceous (~110–90 Ma).

From the Huoshiling to Shahezi and Yingcheng stages, the basin evolved from deeper, humid freshwater to shallower, semi-arid and more brackish conditions, with a gradual decline in water-column reducing capacity. High TOC values (>2 wt%) correlate positively with redox-sensitive elements (V, Ni, Cr, V/Cr, Ni/Co) and with humid-climate indicators (Cu enrichment, high paleoclimate index, low Sr/Cu < 6), suggesting that strongly reducing and semi-humid conditions favored the formation of high-quality source rocks. Paleosalinity proxies (Sr, Sr/Ba, Sr/Ca) show weaker

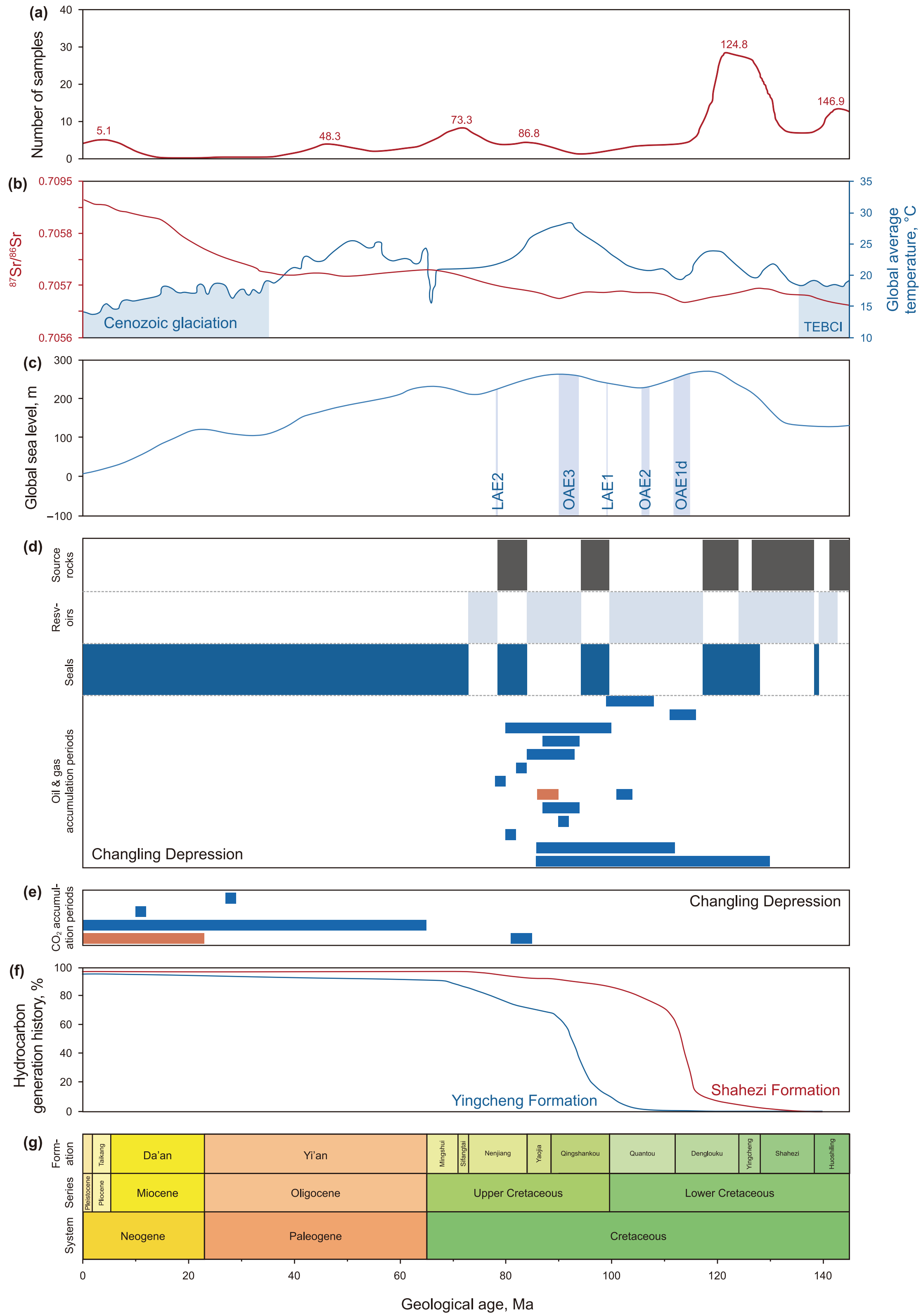

Fig. 11. Multi-sphere interactions and hydrocarbon system evolution in the Changling Fault Depression, Songliao Basin. **(a)** Tectonic chronology (Cheng et al., 2020). **(b)** Global average temperature curve (Scotese, 2021) and global marine $^{87}Sr/^{86}Sr$ curve (McArthur et al., 2020). **(c)** Global sea-level variations (Boulila et al., 2021) and regional transgression events (Wu et al., 2024). **(d)** Source-reservoir-seal systems and hydrocarbon charging stages, modified from Yu et al. (2013). **(e)** CO_2 charging episodes. **(f)** The hydrocarbon generation history curve of Yingcheng Formation and Shahezi Formation, modified from Huang et al. (2012). **(g)** Chronostratigraphic framework of the Songliao Basin. Note on colored blocks and legend: In panels (b)–(e) the colored blocks are time intervals referenced to the stratigraphic/time axis shown in panel (g); the horizontal length of each block corresponds to its duration on the panel(g) time axis. The meaning of each color is indicated by the left-side panel headings and by the legend box plotted on the figure. For clarity, the primary color key used in panels (d)–(e) is: the first charging period is represented in blue, and the second charging period is represented in orange.

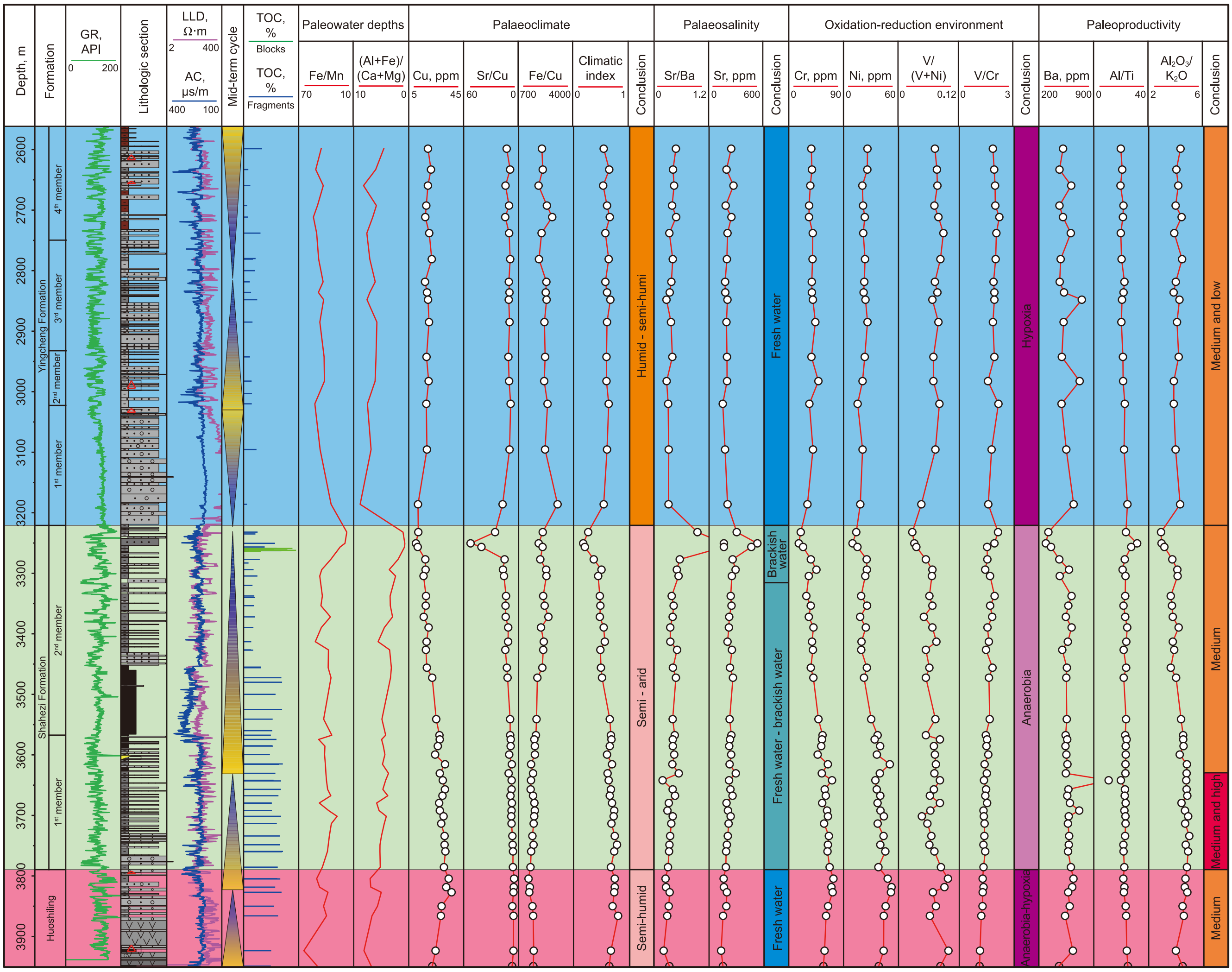

Fig. 12. The elemental signatures and paleoenvironmental reconstruction of Lower Cretaceous lacustrine hydrocarbon source rocks in Well SL3, Changling Fault Depression, Songliao Basin. Modified from Li et al. (2017).

relationships, indicating a limited role of salinity in controlling organic-matter preservation.

Multiple black shale intervals in the basin correlate with global OAE episodes, including the Denglouku Formation Member 4 (OAE1d equivalent), Quantou Formation Member 3 (OAE2 equivalent), and Qingshankou Formation Members 2–3 (OAE3 equivalent) (Fig. 11(c)). Notably, large-scale marine incursions during Qingshankou Formation Member 1 and Nenjiang Formation Member 2 triggered lacustrine anoxic events (LAE1 and LAE2), creating optimal organic enrichment conditions that produced the most prolific hydrocarbon source intervals (Fig. 11(c)) (Wu et al., 2024). The Changling Fault Depression's gas accumulations primarily originate from coal-bearing Shahezi Formation source rocks, whose deposition was influenced by organic-rich volcanic ash sedimentation following early magmatic eruptions, concurrent with climatic temperature fluctuations.

The Cretaceous organic-rich shales exhibit exceptional hydrocarbon generation potential, a characteristic arising from atmosphere-hydrosphere-lithosphere interactions (Zhang et al., 2024b; Zhu et al., 2024). Proven natural gas reserves in synchronous rift volcaniclastic reservoirs reach 156.4 trillion cubic feet, attesting to the superior petroleum geological conditions (Liu et al., 2023a). This resource endowment reflects synergistic controls among tectonic subsidence rhythms, magmatic-thermal perturbations, and climate-driven biogeochemical cycles (Chen et al., 2023), establishing the Songliao Basin as a global archetype for understanding continental rift basin petroleum systems under greenhouse climate regimes.

5.3. Jointly controlled by tectonics, transgression, and climatic evolution

The formation of petroleum systems exhibits distinct tectonic-climatic coupling characteristics, fundamentally reflecting the synergistic interplay between Earth's endogenic and exogenic dynamic systems during specific geological periods (Scotese, 2021; Jin et al., 2023). Endogenic processes which include plate drift, continental rifting-collision, orogenesis, and volcanism are directly govern regional paleogeographic evolution and eustatic variations, thereby orchestrating the spatiotemporal configuration of critical petroleum system elements (source rocks, reservoirs, and caprocks) (Ming et al., 2009; Meng et al., 2014; Liu et al., 2023b).

In the Songliao Basin, two pivotal volcanic episodes exerted decisive controls on petroleum system development (Fig. 11): (i) Early Cretaceous (146.9–124.8 Ma) steep-angle, low-velocity subduction of the Pacific Plate triggered large-scale volcanism coinciding with >100 m global sea-level rise and stable 15 °C climatic conditions, forming premium volcanic reservoirs exemplified by the Yingcheng, Shahezi, and Huoshiling Formations. (ii) Late Cretaceous to present (73.3–5.1 Ma) shallow-angle, accelerated subduction facilitated mantle-derived magma emplacement and CO_2 charging. Notably, limited CO_2 degradation during this phase, coupled with progressive sea-level fall and global cooling, established unique gas preservation conditions.

The two major marine transgressions synchronously responded to global eustatic cycles (Liu et al., 2011; Bai et al., 2023; Wang et al., 2024a). This tripartite coupling mechanism, comprising tectonic activation, sea-level fluctuation, and climatic variation, not only shaped pore evolution in volcanic reservoirs but also determined the spatial distribution and resource abundance of petroleum systems by modulating anoxic event frequency and organic carbon burial efficiency (Bjerrum and Canfield, 2004; Irwin et al., 1977). Specifically, Early Cretaceous hydrothermal alteration enhanced secondary porosity in volcaniclastics through zeolitization and chloritization, while Late Cretaceous tectonic inversion created fracture networks that optimized reservoir permeability (Liu et al., 2017b). The temporal coincidence of enhanced organic productivity during oceanic anoxic events (OAEs) and optimal reservoir diagenesis during tectonic quiescence periods created a unique configuration, positioning the Songliao Basin as a global benchmark for studying continental rift petroleum systems under greenhouse climate regimes.

Based on the geochemical data from the Lower Cretaceous source rocks in Well SL3, the paleoenvironmental evolution profile of the study area during the Early Cretaceous were reconstructed (Fig. 12). The reconstruction indicates that from the Huoshiling to the Shahezi and Yingcheng depositional stages, the Changling Fault Depression experienced a progressive transition from deep to shallow water depth, from humid to semi-arid climate conditions, from freshwater to brackish environments, and from increasing to decreasing water column reducing capacity (Li et al., 2017). Overall, the paleoenvironment during the Shahezi and Yingcheng stages showed significant stratified variation, which directly controlled the heterogeneity in hydrocarbon generation potential across different source rock intervals.

A significant positive correlation is observed between total organic carbon (TOC) content and redox-sensitive elements such as Cr, Ni, V, Ni/Co, and V/Cr (Fig. 13(a)–(e)). Samples with TOC greater than 2.0% are notably enriched in V, Ni, and Cr (Fig. 13(a)–(c)), indicating that the formation of high-quality Lower Cretaceous source rocks was primarily controlled by strongly reducing water column conditions. Meanwhile, TOC also correlates well with paleoclimate-sensitive indicators, including Cu, Fe/Cu, and Sr/Cu ratios (Fig. 13(f)–(i)), as well as the paleoclimate index (Li et al., 2017). Most samples with TOC > 2.0% are Cu-enriched (Fig. 13(f)), show paleoclimate index values above 0.7, and Sr/Cu ratios below 6 (Fig. 13(i)), all pointing to a semi-humid to humid climate regime. In contrast, TOC shows a weaker correlation with paleosalinity indicators such as Sr, Sr/Ba, and Sr/Ca (Fig. 13(j)–(l)), suggesting that paleosalinity had a limited impact on the development of high-quality source rocks in this region (Li et al., 2017). These observations collectively demonstrate that redox conditions and paleoclimate were the dominant environmental factors controlling source rock quality in the Lower Cretaceous.

There is a strong coupling relationship among paleoproductivity, redox conditions, and paleoclimate, which directly influenced organic matter enrichment (Wang et al., 2024b; Zhao et al., 2025). TOC content is positively correlated with paleoproductivity indicators such as Al_2O_3/K_2O, Al/Ti, and Ba concentrations (Fig. 13(m)–(o)). Source rocks from the Shahezi and Huoshiling formations display higher paleoproductivity levels (Figs. 11(d) and 12), while those from the Yingcheng Formation exhibit relatively lower values.

During the early depositional stage (Shahezi Formation), tectonic activity and volcanism were relatively weak, resulting in limited accommodation space and shallow water depths. Under humid to semi-humid climatic conditions, intensified river inflow delivered abundant terrestrial organic matter, primarily from higher plants. However, the injection of large volumes of freshwater reduced salinity and weakened water column stratification, leading to poor preservation conditions and consequently low organic matter abundance (Fig. 14(a)). In contrast, during the Yingcheng Formation stage, enhanced rifting and volcanic activity expanded the basin accommodation space and deepened the water column. Inputs of volcanic materials stimulated the proliferation of algae and other lower aquatic organisms. Under semi-arid conditions, terrestrial input decreased, while higher salinity strengthened stratification and reducing capacity, greatly improving organic matter preservation (Fig. 14(b)). The co-evolution of lake basin settings under tectonic control, coupled with volcanic influence, jointly regulated the spatial and temporal distribution of high-quality source rocks in the study area.

5.4. Integrated multi-sphere coupling: mechanisms and evidences

The interactions among the lithosphere, atmosphere, and hydrosphere are key to understanding the spatiotemporal distribution of both natural gas and CO_2 in the Changling Fault Depression. To strengthen the coupling discussion, we integrate the available geochemical, isotopic, and paleoenvironmental evidence into three major pathways that reveal how multi-spherical processes jointly influenced gas generation, migration, and preservation.

Volcanic and magmatic activities during the Huoshiling–Yingcheng periods supplied abundant heat and nutrient-rich detritus to the lacustrine system. These pulses enhanced primary productivity and, combined with stratification and rapid burial, promoted organic carbon accumulation and preservation. This interpretation is supported by elevated TOC contents and higher V/Cr and Sr/Cu ratios observed in the Yingcheng Formation (Figs. 12 and 13), indicating a more reducing and saline depositional environment compared with the Shahezi Formation.

Episodes of mantle-derived CO_2 injection, identified by $\delta^{13}C_{CO_2}$ values ranging from −18.9‰ to −0.6‰ and by deep CO_2 enrichment zones (2.66–4.55 km), altered the local carbon equilibrium, redox state, and carbonate precipitation potential (Section 4.2). These CO_2 pulses, likely linked to syn-magmatic degassing, influenced both the geochemical environment of the source rocks and the diagenetic evolution of reservoirs, thus modifying gas accumulation efficiency and phase distribution.

Tectonic inversion and episodic fault reactivation not only regulated hydrocarbon generation timing but also determined the connectivity between deep mantle reservoirs and shallower sedimentary systems. Deep, high-permeability faults served as conduits for upward migration of mantle-sourced CO_2 and He, while shallower carrier beds facilitated lateral migration and trapping of thermogenic CH_4. This complementary spatial pattern is evident from the planar distribution of CH_4 and CO_2 (Fig. 6) and the noble-gas enrichments near deep faults (Supplementary Material). The interplay between vertical and lateral migration establishes the structural foundation for the observed partitioning of CH_4-rich and CO_2-rich zones (Fig. 11).

This synthesis reinforces the integrated nature of the system, showing that lithospheric tectono-magmatic activities provided both the energy and materials driving hydrocarbon generation and

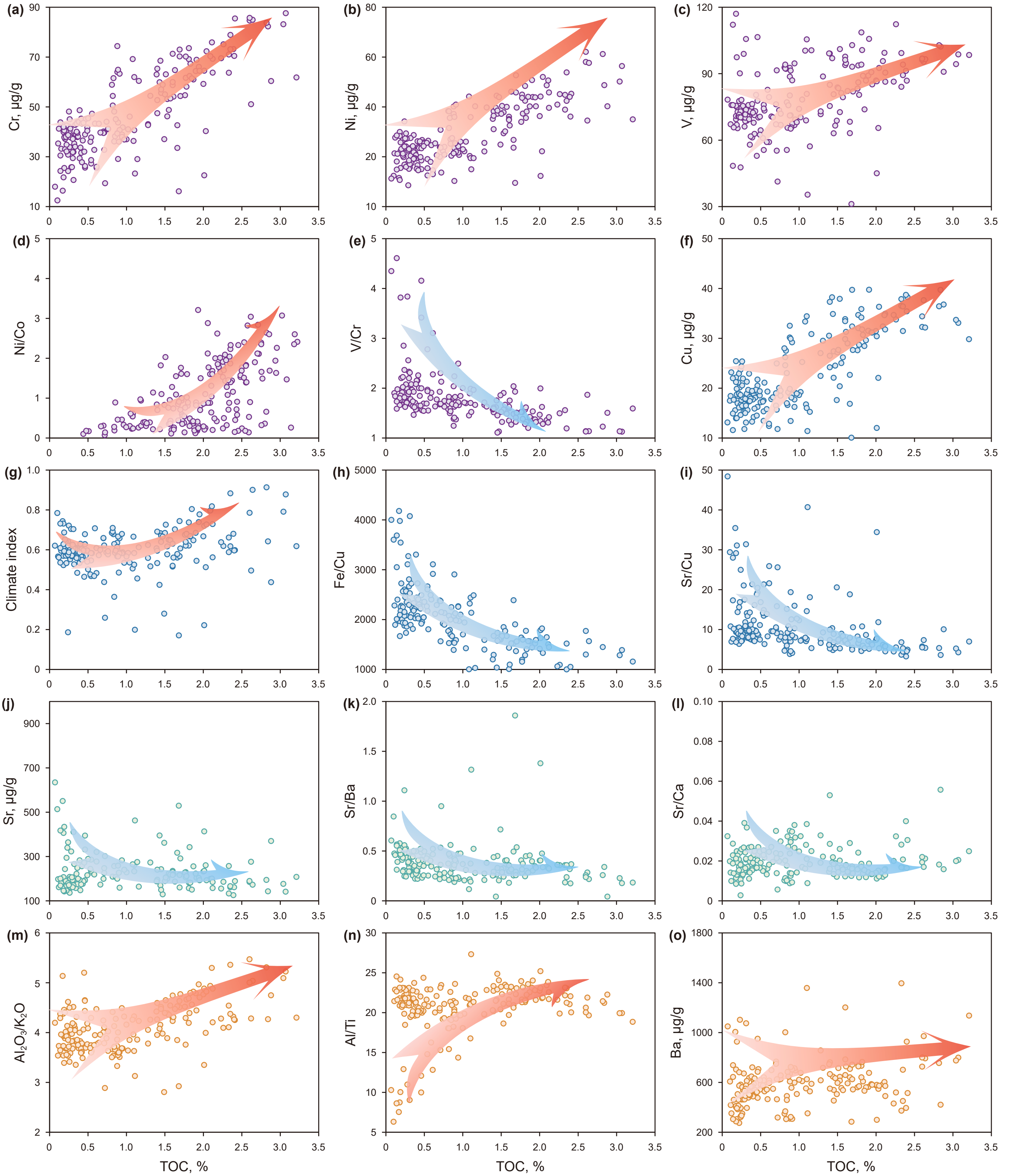

Fig. 13. Relationships between element contents (or their ratios) and TOC in Lower Cretaceous hydrocarbon source rocks of Changling Fault Depression, Songliao Basin. This integrated analytical framework encompasses four paleoenvironmental indicator modules: redox-sensitive elements ((**a**) Cr, (**b**) Ni, (**c**) V concentrations) with their diagnostic ratios (**d**) Ni/Co and (**e**) V/Cr for redox conditions; paleoclimate proxies including (**f**) Cu concentration, (**g**) Paleoclimate index, and elemental coupling ratios (**h**) Fe/Cu and (**i**) Sr/Cu; paleosalinity indicators featuring (**j**) Sr concentration combined with (**k**) Sr/Ba and (**l**) Sr/Ca ratios; and paleoproductivity parameters demonstrated by (**m**) Al_2O_3/Ti, (**n**) Al/Ti ratios, and (**o**) Ba concentration.

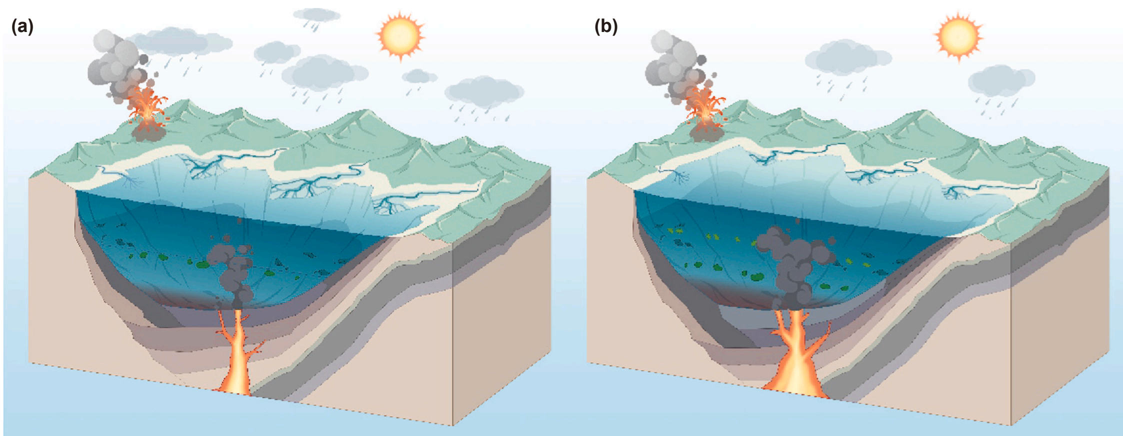

Fig. 14. Schematic model of tectonic-climatic-sedimentary interactions. (**a**) Rifting and volcanic activity are weak, resulting in limited lacustrine accommodation space and shallow water depth. (**b**) Enhanced rifting and volcanic activity lead to rising base level, increasing sedimentary accommodation space and deepening of the water body.

CO_2 enrichment, while hydrospheric and atmospheric factors modulated organic preservation and post-generation redistribution.

5.5. Comparison of multi-sphere interactions in Songliao and other basins

The formation and evolution of hydrocarbon systems in rift basins are increasingly recognized as outcomes of dynamic interactions among internal Earth processes, climatic conditions, and sedimentary environments (Liu et al., 2024; Zhang et al., 2024b; Jiang et al., 2025b; Jiang and Liu, 2025; Wang et al., 2025). A comparative analysis of the Songliao Basin, the North Sea Basin, and the Bohai Bay Basin highlights both the diversity and commonality of multi-sphere interactions under different tectonic and climatic regimes (Hao and Chen, 2024; Shan et al., 2023; Xie et al., 2024; Zhao et al., 2025; Zhu et al., 2024).

In the Songliao Basin, the development of petroleum systems was controlled by two distinct episodes of Pacific Plate subduction (Chen et al., 2017; Li et al., 2019). The Early Cretaceous stage involved steep-angle subduction, large-scale volcanism, and widespread thermal activity, while the Late Cretaceous stage was dominated by shallower subduction that facilitated CO_2 migration from mantle sources (Cao et al., 2018; Liu et al., 2018; Liu et al., 2023a; Shan et al., 2023). These internal processes coincided with global climate stability and sea level rise during the Early Cretaceous, and with sea level fall and cooling during the Late Cretaceous. The combined influence of tectonic activity, climate variation, and sea level change created favorable conditions for hydrocarbon generation and preservation (Zhang et al., 2024b). Oceanic anoxic events promoted organic carbon accumulation, while hydrothermal alteration and faulting enhanced secondary porosity and permeability in volcaniclastic reservoirs (Li et al., 2018; Liu et al., 2023; Zhang et al., 2024b). This convergence of processes resulted in a unique match between source rock development, reservoir formation, and hydrocarbon charging periods.

In the North Sea Basin, the petroleum systems evolved through multiple phases of crustal extension and thermal subsidence from the Paleozoic to the Cenozoic (Zhu et al., 2024). Deep mantle activity and slab rollback shaped the architecture of basin, while surface climate patterns and marine transgressions controlled source rock deposition (Zhu et al., 2024). The Jurassic and Cretaceous successions, including the Draupne and Kimmeridge formations, were formed through the overlap of tectonic subsidence, anoxic bottom waters, and regional shale deposition. Although the North Sea lacks significant volcanic activity, its long-term geodynamic and climatic interactions show a different but equally effective form of multi-sphere coupling. Both the Songliao and North Sea basins share a critical characteristic which is temporal alignment between hydrocarbon generation and reservoir development.

The Bohai Bay Basin, especially the Kongdian 2nd Member of the Cangdong Sag, represents another variation of sphere interaction. The hydrocarbon accumulation of basin follows a layered configuration controlled by lithospheric deformation, hydrological evolution, biological productivity, and sediment supply (Zhao et al., 2025). This resulted in a vertically differentiated system, with microbial gas in the upper zone, oil in the middle, and deep thermogenic gas at the bottom (Zhao et al., 2025). Unlike the temporally synchronized system of the Songliao Basin, the Bohai Basin case shows how multiple petroleum systems can coexist in a stratified structure formed by repeated tectonic and climatic cycles. Despite differences in lithology and burial history, both basins exhibit the importance of vertical structural control and fluid partitioning across geological time.

Together, these comparisons demonstrate that although the geological expressions of multi-sphere interactions vary, the underlying principles remain consistent. The coordination of tectonic events, climatic phases, and sedimentary dynamics is a powerful driver of petroleum system evolution (Shan et al., 2023; Hao and Chen, 2024; Xie et al., 2024; Zhu et al., 2024; Zhao et al., 2025). The Songliao Basin, with its volcanic reservoir systems and deep CO_2 inputs, offers a globally relevant case for understanding greenhouse-driven hydrocarbon accumulation in continental rift settings. Recent studies have emphasized that hydrocarbon generation and enrichment represent a complex geodynamic process involving multi-spheric material cycles, energy transfer, and coupled evolutionary mechanisms. Research in this direction is still in its early stage and requires integrated approaches that combine deep lithospheric dynamics, multi-spheric interactions, petroleum system evolution, and emerging tools such as machine-learning–based predictive analysis. The recently proposed multi-spheric interaction-driven hydrocarbon formation theory (Zhu et al., 2025) further highlights the necessity of linking deep Earth processes with surface environmental responses to fully understand spatiotemporal variations in hydrocarbon systems. The findings from the Changling Fault Depression are consistent

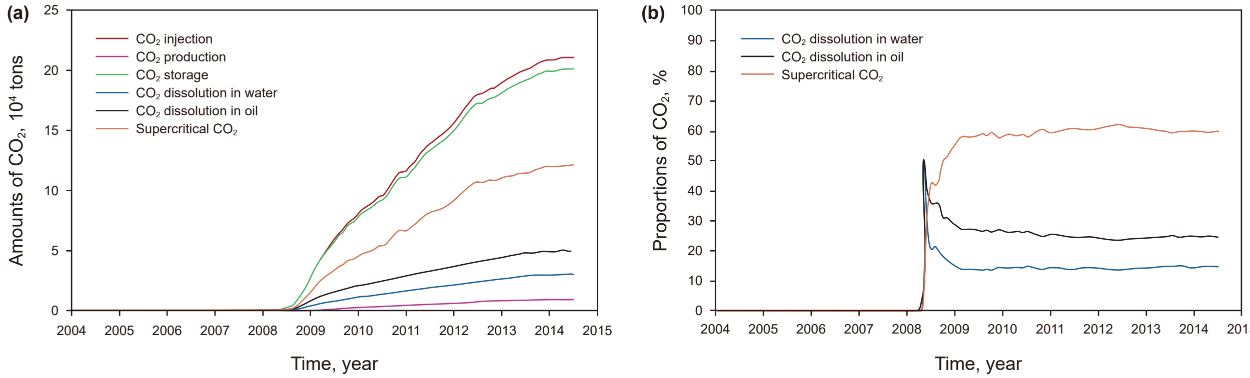

Fig. 15. Amounts **(a)** and proportions **(b)** of CO_2 trapped in various forms in the H-59 block, modified from Zhang et al. (2016).

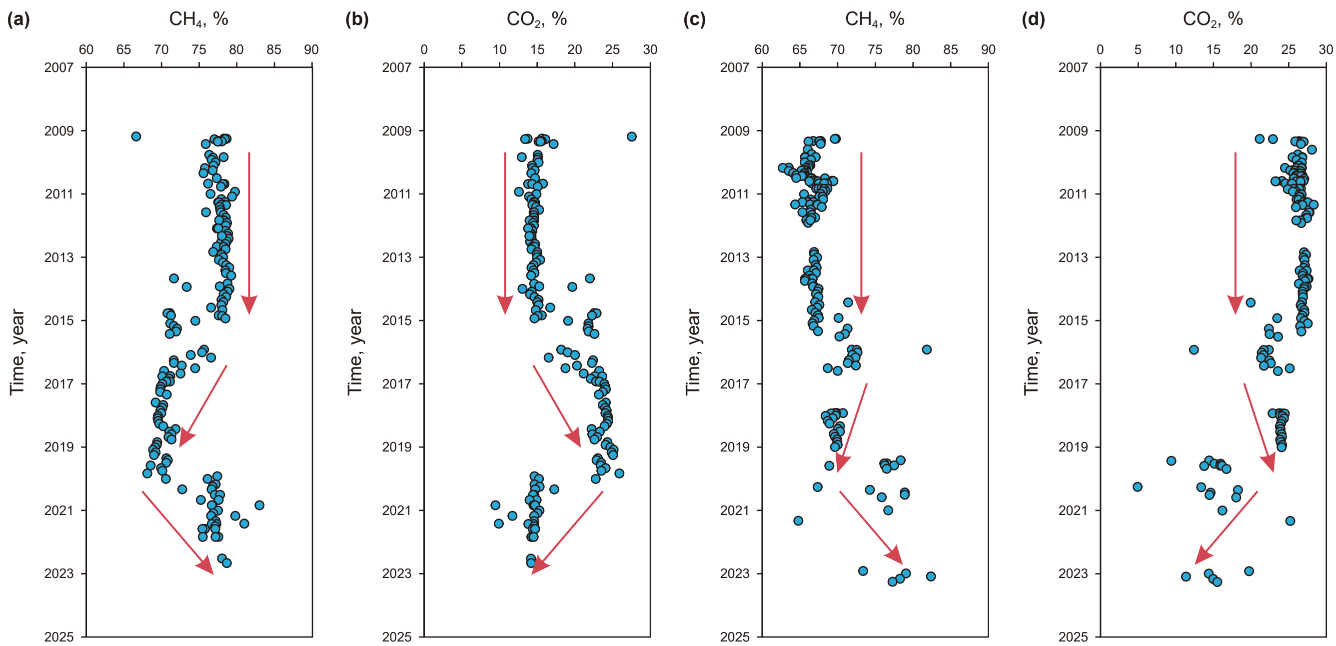

Fig. 16. Temporal variation of gas content in the Changling Fault Depression, Songliao Basin. **(a)** CH_4 and **(b)** CO_2 in Well CS1-1. **(c)** CH_4 and **(d)** CO_2 in Well CS103.

with this emerging framework, while also providing basin-scale evidence that complements observations from other volcanic-rifted systems in East Asia.

5.6. Implications for CO_2 sequestration

A representative case study from the H-59 block, located in the western part of the Daqingzi subregion within the central Changling Fault Depression of the southern Songliao Basin, was used to validate the applicability of the integrated CO_2 sequestration potential area (Fig. 1(b)). The block covers an area of approximately 3.1 km^2, with an estimated original oil in place of about 1.6 million tonnes. The primary oil-bearing interval is hosted in the Qingshankou Formation (Qing I-III members), which is overlain by a regionally continuous 500–550 m thick mudstone caprock. The reservoir is oil-dominated (Dong et al., 2014; Liu et al., 2017b; Huo et al., 2020; Liu et al., 2023a).

To date, a total of 210,800 tonnes of CO_2 has been injected into the reservoir, resulting in cumulative oil production of 126,400 tonnes (Zhang et al., 2016) (Fig. 15(a)). The oil recovery factor during the CO_2 injection stage increased from 5% to 14.7%. Concurrently, cumulative water injection and production volumes reached 109,600 and 119,300 tonnes, respectively, while 9600 tonnes of CO_2 have been recovered (Fig. 15(a)). The current effective CO_2 storage volume is estimated at 201,200 tonnes (Zhang et al., 2016).

Reservoir simulation and material balance analyses indicate the partitioning of stored CO_2 as follows (Zhang et al., 2016) (Fig. 15(b)): 42.68%–60.15% (~121,000 tonnes) is trapped in a supercritical state, 24.85%–41.8% (~50,000 tonnes) is dissolved in residual oil, and the remaining 15% (~30,200 tonnes) is dissolved in formation water. Based on the reservoir's physical characteristics and current performance, the estimated maximum effective storage potential is 263,700 tonnes, leaving a residual capacity of 62,500 tonnes (Zhang et al., 2016).

These results confirm that the geological setting of the Changling Fault Depression is highly favorable for long-term CO_2 sequestration, and that the integrated evaluation model can effectively predict high-potential zones with substantial CO_2 storage capacity (Du et al., 2016; Zhang et al., 2016; Dou et al., 2023; Song et al., 2023; Wang, 2023; Wang et al., 2023). The H-59 case thus provides real-world validation for the practical applicability of models.

5.7. Limitation of data

Significant temporal variations in gas composition were identified during the analysis of natural gas and CO_2 distribution characteristics. Comparative longitudinal analysis of gas samples collected across different drilling years revealed distinct compositional evolution patterns: CH_4 concentrations exhibited a three-phase stable-decline-rise trend (Fig. 16(a) and (c)), while CO_2 displayed an inverse stable-rise-decline trajectory (Fig. 16(b) and (d)), with final steady-state compositions remaining below initial production levels. This temporal dependency implies dynamic compositional re-equilibration during gas field development.

It is hypothesized that before production began, the reservoir maintained a natural equilibrium where CH_4 with a molecular weight of 16.04 was concentrated in the upper part and CO_2 with a molecular weight of 44.01 was enriched in the lower part of the reservoir. This balance may have been disturbed by continued extraction but other mechanisms could also be involved. Engineering factors such as gas injection or pressure maintenance were ruled out through audits of operational protocols. The observed compositional variations are therefore more likely caused by pressure decline and fluid redistribution during production activities.

6. Conclusions

Natural gas in the Changling Fault Depression is dominated by CH_4 (60%–97.4%) with low C_2+ contents, while $\delta^{13}C_1$ values (−56.8‰ to −1.7‰) indicate mixed thermogenic and abiogenic origins locally influenced by coal-derived gas. CO_2 displays ultra-high concentrations (up to 99.45%) and $\delta^{13}C_{CO_2}$ values (−18.9‰ to −0.6‰) confirming a predominant inorganic mantle-derived source with minor organic input in Daerhan. Carbon isotope reversals and fractionation patterns reflect multi-source mixing and post-accumulation alteration.

Spatially, CH_4 preferentially accumulates in volcanic reservoirs of the Quantou and Yingcheng Formations, whereas CO_2-rich zones (>80%) dominate the eastern Changshen area, complementary to CH_4 distributions. N_2, H_2, and He enrichments are fault-controlled, indicating deep fluid connectivity through basement structures. Hydrocarbon accumulation followed two pathways: near-source vertical migration via Shahezi faults and lateral migration along Yingcheng carrier beds. Mantle-derived CO_2 migrated upward along reactivated basement faults during Late Cretaceous–Paleogene magmatism, while later tectonic inversion (40–10 Ma) enhanced reservoir preservation by sealing fractures and generating microporosity in volcaniclastics.

Integrating these results, we propose a tectonic-climatic-sedimentary multi-sphere coupling model, wherein lithospheric processes (Pacific Plate subduction, basement faulting, and volcanism) controlled reservoir architecture and CO_2 charging; hydrospheric lacustrine fluctuations and atmospheric Ferrel circulation modulated organic enrichment via climate-sedimentation coupling; and biospheric productivity governed organic burial efficiency enhanced by volcanic ash. Paleoenvironmental evolution from the Huoshiling to Yingcheng stages-characterized by shallowing lake levels, semi-arid transition, and decreasing redox capacity-regulated source rock quality, with the Shahezi Formation showing stronger productivity and hydrocarbon generation potential.

This synthesis reveals that hydrocarbon enrichment in the Changling Fault Depression results from the interplay of magmatic, climatic, and depositional factors across multiple Earth spheres. The proposed model provides a new conceptual framework for understanding gas-CO_2 coexistence in volcanic basins and supports deep unconventional exploration and carbon-neutral strategies through integrated CO_2 sequestration-reservoir management approaches.

CRediT authorship contribution statement

Ming-Ming Jiang: Writing – review & editing, Writing – original draft, Software, Methodology, Funding acquisition, Conceptualization. **Si-Shuo Zhou:** Writing – original draft, Visualization. **Xin Yan:** Writing – original draft, Data curation. **Quan-You Liu:** Supervision, Project administration, Funding acquisition.

Declaration of competing interest

The authors declare that they have no known competing financial interests or personal relationships that could have appeared to influence the work reported in this paper.

Acknowledgments

This research was supported by the National Natural Science Foundation of China (Grant Nos. 42488101, 42302146, U20B6001, 42141021), the Natural Science Foundation of Inner Mongolia (2025YQ008), the Peking University-BHP Carbon and Climate Wei-Ming PhD Scholars Program (WM202503), the open research project of State Key Laboratory of Acoustics and Marine Information, Chinese Academy of Sciences (No. SKLA202412), the 2024 AAPG Foundation Grants-in-Aid, and China National Petroleum Corporation & Peking University Basic Research Project (JTGS-2022-JS-327). Additionally, we extend our appreciation to the reviewers for their valuable contributions towards improving this paper.

Appendix A. Supplementary data

Supplementary data to this article can be found online at https://doi.org/10.1016/j.petsci.2026.02.006.

References

Alcott, L.J., Walton, C., Planavsky, N.J., et al., 2024. Crustal carbonate build-up as a driver for Earth's oxygenation. Nat. Geosci. 17 (5), 458–464. https://doi.org/10.1038/s41561-024-01417-1.

Bai, L., Liu, B., Fu, X., et al., 2023. A new method for evaluating the oil mobility based on the relationship between pore structure and state of oil. Geosci. Front. 14 (6), 101684. https://doi.org/10.1016/j.gsf.2023.101684.

Barclay, R.S., McElwain, J.C., Sageman, B.B., 2010. Carbon sequestration activated by a volcanic CO_2 pulse during Ocean Anoxic Event 2. Nat. Geosci. 3 (3), 205–208. https://doi.org/10.1038/ngeo757.

Bernard, B.B., Brooks, J.M., Sackett, W.M., 1978. Light hydrocarbons in recent Texas continental shelf and slope sediments. J. Geophys. Res., Oceans 83 (C8), 4053–4061. https://doi.org/10.1029/JC083iC08p04053.

Bjerrum, C.J., Canfield, D.E., 2004. New insights into the burial history of organic carbon on the early Earth. G-cubed 5 (8), 2004GC000713. https://doi.org/10.1029/2004GC000713.

Boscolo-Galazzo, F., Crichton, K.A., Ridgwell, A., et al., 2021. Temperature controls carbon cycling and biological evolution in the ocean twilight zone. Science 371 (6534), 1148–1152. https://doi.org/10.1126/science.abb6643.

Boulila, S., Haq, B.U., Hara, N., et al., 2021. Potential encoding of coupling between Milankovitch forcing and Earth's interior processes in the Phanerozoic eustatic sea-level record. Earth Sci. Rev. 220, 103727. https://doi.org/10.1016/j.earscirev.2021.103727.

Bowring, S.P.K., Jones, M.W., Ciais, P., et al., 2022. Pyrogenic carbon decomposition critical to resolving fire's role in the Earth system. Nat. Geosci. 15 (2), 135–142. https://doi.org/10.1038/s41561-021-00892-0.

Brand, U., Posenato, R., Came, R., et al., 2012. The end-Permian mass extinction: A rapid volcanic CO_2 and CH_4-climatic catastrophe. Chem. Geol. 322–323, 121–144. https://doi.org/10.1016/j.chemgeo.2012.06.015.

Brune, S., Williams, S.E., Müller, R.D., 2017. Potential links between continental rifting, CO_2 degassing and climate change through time. Nat. Geosci. 10 (12), 941–946. https://doi.org/10.1038/s41561-017-0003-6.

Cao, Z., Lin, C., Dong, C., et al., 2018. Impact of sequence stratigraphy, depositional facies, diagenesis and CO_2 charge on reservoir quality of the lower cretaceous Quantou Formation, Southern Songliao Basin. China. Mar. Petrol. Geol. 93, 497–519. https://doi.org/10.1016/j.marpetgeo.2018.03.015.
Chen, H., Xia, Q.K., Ingrin, J., et al., 2017. Heterogeneous source components of intraplate basalts from NE China induced by the ongoing Pacific slab subduction. Earth Planet Sci. Lett. 459, 208–220. https://doi.org/10.1016/j.epsl.2016.11.030.
Chen, H., Xu, X., Fang, C., et al., 2021. Differences in the temperature dependence of wetland CO_2 and CH_4 emissions vary with water table depth. Nat. Clim. Change 11 (9), 766–771. https://doi.org/10.1038/s41558-021-01108-4.
Chen, Z., Ding, Z., Yang, S., et al., 2023. Strong coupling between carbon cycle, climate, and weathering during the Paleocene-Eocene thermal maximum. Geophys. Res. Lett. 50 (9), e2023GL102897. https://doi.org/10.1029/2023GL102897.
Cheng, Y., Wang, S., Zhang, T., et al., 2020. Regional sandstone-type uranium mineralization rooted in Oligo–Miocene tectonic inversion in the Songliao Basin, NE China. Gondwana Res. 88, 88–105. https://doi.org/10.1016/j.gr.2020.08.002.
Dai, J., Ni, Y., Huang, S., et al., 2014. Significant function of coal-derived gas study for natural gas industry development in China. Nat. Gas Geosci. 25 (1), 1–22. https://doi.org/10.11764/j.issn.1672-1926.2014.01.0001 (in Chinese).
Dai, J., 1992. Identification of various genetic natural gases. China Offshore Oil Gas (Geol.) 6 (1), 11–19.
Dong, T., He, S., Wang, D., et al., 2014. Hydrocarbon migration and accumulation in the Upper Cretaceous Qingshankou Formation, Changling Sag, southern Songliao Basin: Insights from integrated analyses of fluid inclusion, oil source correlation and basin modelling. J. Asian Earth Sci. 90, 77–87. https://doi.org/10.1016/j.jseaes.2014.04.002.
Dou, L., Sun, L., Lyu, W., et al., 2023. Trend of global carbon dioxide capture, utilization and storage industry and challenges and countermeasures in China. Petrol. Explor. Dev. 50 (5), 1246–1260. https://doi.org/10.1016/S1876-3804(23)60463-X.
Du, S., Su, X., Xu, W., 2016. Assessment of CO_2 geological storage capacity in the oilfields of the Songliao Basin, northeastern China. Geosci. J. 20 (2), 247–257. https://doi.org/10.1007/s12303-015-0037-y.
Etiope, G., Nakada, R., Tanaka, K., et al., 2011. Gas seepage from Tokamachi mud volcanoes, onshore Niigata Basin (Japan): Origin, post-genetic alterations and CH_4–CO_2 fluxes. Appl. Geochem. 26 (3), 348–359. https://doi.org/10.1016/j.apgeochem.2010.12.008.
Fu, X., Sha, W., Wang, L., et al., 2010. Distribution law of mantle-origin CO_2 gas reservoirs and its controlling factors in Songliao Basin. J. Jilin Univ. (Earth Sci. Ed.) 40 (2), 253–263. https://doi.org/10.3724/SP.J.1231.2010.06586 (in Chinese).
Fu, G., Wu, W., Li, N., 2014. Controlling effect of three major faults on gas accumulation in the Xujiaweizi faulted depression, Songliao Basin. Nat. Gas. Ind. B. 1 (2), 159–164. https://doi.org/10.1016/j.ngib.2014.11.006.
Fu, X., Su, X., Gong, L., et al., 2023. Control of faults and fractures on shale oil enrichment. Geoenergy Sci. Eng. 228, 212080. https://doi.org/10.1016/j.geoen.2023.212080.
Gao, J., Liu, J., Hilton, D.R., et al., 2017. The chemical and isotopic compositions of volatiles in magmatic hydrothermal fluids beneath the Songliao Basin, northeastern China. Chem. Geol. 465, 11–20. https://doi.org/10.1016/j.chemgeo.2017.05.015.
Hao, Z., Chen, Y., 2024. Research progresses and prospects of multi-sphere compound extremes from the Earth System perspective. Sci. China Earth Sci. 67 (2), 343–374. https://doi.org/10.1007/s11430-023-1201-y.
Hemingway, J.D., Hilton, R.G., Hovius, N., et al., 2018. Microbial oxidation of lithospheric organic carbon in rapidly eroding tropical mountain soils. Science 360 (6385), 209–212. https://doi.org/10.1126/science.aao6463.
Huang, H., Yang, J., Yang, Y., et al., 2004. Geochemistry of natural gases in deep strata of the Songliao Basin, NE China. Int. J. Coal Geol. 58 (4), 231–244. https://doi.org/10.1016/j.coal.2003.12.004.
Huang, W., Lu, S., Jiang, T., et al., 2012. Accumulation periods of deep gas reservoirs in Changling Fault Depression. J. Jilin Univ. (Earth Sci. Ed.) 42 (1), 105–111. https://doi.org/10.1177/076737010001500103 (in Chinese).
Huang, Y., Ciais, P., Luo, Y., et al., 2021. Tradeoff of CO_2 and CH_4 emissions from global peatlands under water-table drawdown. Nat. Clim. Change 11 (7), 618–622. https://doi.org/10.1038/s41558-021-01059-w.
Huo, Z., Hao, S., Liu, B., et al., 2020. Geochemical characteristics and hydrocarbon expulsion of source rocks in the first member of the Qingshankou Formation in the Qijia-Gulong Sag, Songliao Basin, Northeast China: Evaluation of shale oil resource potential. Energy Sci. Eng. 8 (5), 1450–1467. https://doi.org/10.1002/ese3.603.
Inguaggiato, S., Mazzini, A., Vita, F., et al., 2018. The Arjuno-Welirang volcanic complex and the connected Lusi system: Geochemical evidences. Mar. Petrol. Geol. 90, 67–76. https://doi.org/10.1016/j.marpetgeo.2017.10.015.
Irwin, H., Curtis, C., Coleman, M., 1977. Isotopic evidence for source of diagenetic carbonates formed during burial of organic-rich sediments. Nature 269 (5625), 209–213. https://doi.org/10.1038/269209a0.
Jenkyns, H.C., 2010. Geochemistry of oceanic anoxic events. G-cubed 11 (3), Q03004. https://doi.org/10.1029/2009GC002788.
Jia, J., Bechtel, A., Liu, Z., et al., 2013. Oil shale formation in the Upper Cretaceous Nenjiang Formation of the Songliao Basin (NE China): Implications from organic and inorganic geochemical analyses. Int. J. Coal Geol. 113, 11–26. https://doi.org/10.1016/j.coal.2013.03.004.
Jiang, M., Liu, Q., 2025. Geochemical characteristics of ultra-deep natural gases. Org. Geochem. 203, 104964. https://doi.org/10.1016/j.orggeochem.2025.104964.
Jiang, M., Jin, Y., Fu, X., et al., 2023. The development of cataclastic bands in high-porosity sandstones: Insights from ring shear experiments. J. Struct. Geol. 175, 104952. https://doi.org/10.1016/j.jsg.2023.104952.
Jiang, M., Fu, X., Wang, Z., 2024. An experimental investigation of the characteristics of cataclastic bands in high-porosity sandstones. GSA Bull. 136, 3069–3084. https://doi.org/10.1130/B36801.1.
Jiang, M., Jin, Y., Fu, X., et al., 2025a. Physical simulation and quantitative characterization of fault zones based on ring-shear experiments. Adv. Geo-Energy Res. 17, 256–266. https://doi.org/10.46690/ager.2025.09.07.
Jiang, M., Liu, Q., Wu, X., et al., 2025b. Advancements in geochemistry and origins of CO_2 in natural gas reservoirs of China. Mar. Petrol. Geol. 173, 107267. https://doi.org/10.1016/j.marpetgeo.2024.107267.
Jiang, M., Jin, Y., Fu, X., et al., 2026. Experimental and analytical approaches to deformation bands: A critical review of laboratory methods, quantitative techniques, and modeling strategies. Earth Sci. Rev. 272, 105343. https://doi.org/10.1016/j.earscirev.2025.105343.
Jin, Z., Wang, X., Wang, H., et al., 2023. Organic carbon cycling and black shale deposition: An Earth System Science perspective. Natl. Sci. Rev. 10 (11), nwad243. https://doi.org/10.1093/nsr/nwad243.
Li, H., Lu, J., Li, R., et al., 2017. Generation paleoenvironment and its controlling factors of Lower Cretaceous lacustrine hydrocarbon source rocks in Changling Depression, South Songliao Basin. Earth Sci. 42 (10), 1774–1786. https://doi.org/10.3799/dqkx.2017.539 (in Chinese).
Li, S., Suo, Y., Li, X., et al., 2018. Microplate tectonics: New insights from micro-blocks in the global oceans, continental margins and deep mantle. Earth Sci. Rev. 185, 1029–1064. https://doi.org/10.1016/j.earscirev.2018.09.005.
Li, S., Suo, Y., Li, X., et al., 2019. Mesozoic tectono-magmatic response in the East Asian ocean-continent connection zone to subduction of the Paleo-Pacific Plate. Earth Sci. Rev. 192, 91–137. https://doi.org/10.1016/j.earscirev.2019.03.003.
Liu, N., Liu, L., Qu, X., et al., 2011. Genesis of authigene carbonate minerals in the Upper Cretaceous reservoir, Honggang Anticline, Songliao Basin: A natural analog for mineral trapping of natural CO_2 storage. Sediment. Geol. 237 (3–4), 166–178. https://doi.org/10.1016/j.sedgeo.2011.02.012.
Liu, Q., Dai, J., Jin, Z., et al., 2016. Abnormal carbon and hydrogen isotopes of alkane gases from the Qingshen gas field, Songliao Basin, China, suggesting abiogenic alkanes? J. Asian Earth Sci. 115, 285–297. https://doi.org/10.1016/j.jseaes.2015.10.005.
Liu, M., Liu, Z., Wu, Y., et al., 2017a. Differences in formation process of tight sandstone gas reservoirs in different substructures in Changling Fault Depression, Songliao Basin, NE China. Petrol. Explor. Dev. 44 (2), 257–264. https://doi.org/10.1016/S1876-3804(17)30028-9.
Liu, R., Liu, Z., Sun, P., et al., 2017b. Shale gas accumulation potential of the Upper Cretaceous Qingshankou Formation in the southeast Songliao Basin, NE China. Mar. Petrol. Geol. 86, 547–562. https://doi.org/10.1016/j.marpetgeo.2017.05.014.
Liu, X., Fu, X., Liu, D., et al., 2018. Distribution of mantle-derived CO_2 gas reservoir and its relationship with basement faults in Songliao Basin, China. J. Nat. Gas Sci. Eng. 56, 593–607. https://doi.org/10.1016/j.jngse.2018.06.040.
Liu, Q., Zhu, D., Meng, Q., et al., 2019. The scientific connotation of oil and gas formations under deep fluids and organic-inorganic interaction. Sci. China Earth Sci. 62 (3), 507–528. https://doi.org/10.1007/s11430-018-9281-2.
Liu, B., He, S., Meng, L., et al., 2021. Sealing mechanisms in volcanic faulted reservoirs in Xujiaweizi extension, northern Songliao Basin, northeastern China. AAPG Bull. 105 (8), 1721–1743. https://doi.org/10.1306/03122119048.
Liu, Z., Dai, L., Li, S., et al., 2022. Earth's surface responses during geodynamic evolution: Numerical insight from the southern East China Sea Continental Shelf Basin, West Pacific. Gondwana Res. 102, 167–179. https://doi.org/10.1016/j.gr.2020.12.011.
Liu, B., Liu, L., Fu, J., et al., 2023a. The Songliao Super Basin in northeastern China. AAPG Bull. 107 (8), 1257–1297. https://doi.org/10.1306/02242321181.
Liu, C., Fu, X., Li, Y., et al., 2023b. Petroleum exploration breakthrough and geological significance in Cretaceous Yingcheng and Denglouku formations of Shuangcheng area, northern Songliao Basin, NE China. Petrol. Explor. Dev. 50 (1), 72–84. https://doi.org/10.1016/S1876-3804(22)60370-7.
Liu, Q., Zhu, D., Meng, Q., et al., 2024. Organic-inorganic interactions in the Earth' s multi-spheres and resources effects. Nat. Gas Geosci. 35 (5), 741–762. https://doi.org/10.11764/j.issn.1672-1926.2024.04.001 (in Chinese).
Lorant, F., Prinzhofer, A., Behar, F., et al., 1998. Carbon isotopic and molecular constraints on the formation and the expulsion of thermogenic hydrocarbon gases. Chem. Geol. 147 (3–4), 249–264. https://doi.org/10.1016/S0009-2541(98)00017-5.
Lou, R., Wang, L., Wang, L., et al., 2022. Characteristics of fluid inclusions and hydrocarbon accumulation period of Huoshiling -Yingcheng Formations in Wangfu fault depression, Songliao Basin, China. J. Petrol. Sci. Eng. 208, 109421. https://doi.org/10.1016/j.petrol.2021.109421.
Lu, Y., Jiang, Y., Wang, W., et al., 2020. Coupling relationship between reservoir diagenesis and hydrocarbon accumulation in Lower Cretaceous Yingcheng Formation of Dongling, Changling Fault Depression, Songliao Basin, Northeast China. China Geol. 3 (1), 1–15. https://doi.org/10.31035/cg2020004.
McArthur, J., Howarth, R., Shields, G., et al., 2020. Strontium isotope stratigraphy. In: Geologic Time Scale 2020. Elsevier, pp. 211–238. https://doi.org/10.1016/B978-0-12-824360-2.00007-3.

Meng, L., Fu, X., Wang, Y., et al., 2014. Internal structure and sealing properties of the volcanic fault zones in Xujiaweizi Fault Depression, Songliao Basin, China. Petrol. Explor. Dev. 41 (2), 165–174. https://doi.org/10.1016/S1876-3804(14)60019-7.

Milkov, A.V., Etiope, G., 2018. Revised genetic diagrams for natural gases based on a global dataset of >20,000 samples. Org. Geochem. 125, 109–120. https://doi.org/10.1016/j.orggeochem.2018.09.002.

Ming, L., Yimin, Z., Xiao, L., et al., 2009. Distribution of petroleum enriched areas, Changling Sag, Southern Songliao Basin. Petrol. Explor. Dev. 36 (4), 413–418. https://doi.org/10.1016/S1876-3804(09)60136-1.

Rizzo, A.L., Pelorosso, B., Coltorti, M., et al., 2018. Geochemistry of noble gases and CO_2 in fluid inclusions from lithospheric mantle beneath Wilcza Góra (lower silesia, southwest Poland). Front. Earth Sci. 6, 215. https://doi.org/10.3389/feart.2018.00215.

Scotese, C.R., 2021. An atlas of Phanerozoic paleogeographic maps: The seas come in and the seas go out. Annu. Rev. Earth Planet Sci. 49 (1), 679–728. https://doi.org/10.1146/annurev-earth-081320-064052.

Shan, X., Mu, H., Liu, Y., et al., 2023. Subaqueous volcanic eruptive facies, facies model and its reservoir significance in a continental lacustrine basin: A case from the Cretaceous in Chaganhua area of southern Songliao Basin, NE China. Petrol. Explor. Dev. 50 (4), 826–839. https://doi.org/10.1016/S1876-3804(23)60431-8.

Song, X., Wang, F., Ma, D., et al., 2023. Progress and prospect of carbon dioxide capture, utilization and storage in CNPC oilfields. Petrol. Explor. Dev. 50 (1), 229–244. https://doi.org/10.1016/S1876-3804(22)60383-5.

Tang, H., Zhao, X., Shao, M., et al., 2017. Reservoir origin and characterization of gas pools in intrusive rocks of the Yingcheng Formation, Songliao Basin, NE China. Mar. Petrol. Geol. 84, 148–159. https://doi.org/10.1016/j.marpetgeo.2017.03.016.

Van Der Meer, D.G., Zeebe, R.E., et al., 2014. Plate tectonic controls on atmospheric CO_2 levels since the Triassic. Proc. Natl. Acad. Sci. USA 111 (12), 4380–4385. https://doi.org/10.1073/pnas.1315657111.

Wang, F., Liao, G., Su, C., et al., 2023. Carbon emission reduction accounting method for a CCUS-EOR project. Petrol. Explor. Dev. 50 (4), 989–1000. https://doi.org/10.1016/S1876-3804(23)60444-6.

Wang, L., Liu, B., Bai, L., et al., 2024a. Pore evolution modeling in natural lacustrine shale influenced by mineral composition: Implications for shale oil exploration and CO_2 storage. Adv. Geo-Energy Res. 13 (3), 218–230. https://doi.org/10.46690/ager.2024.09.07.

Wang, X., Dong, L., Li, T., et al., 2024b. Reconstructing redox landscape with coupled nitrogen-sulfur isotopes: A case study from Middle-Late Triassic Chang 7 Member of the Yanchang Formation in the Ordos Basin (North China). G-cubed 25 (8), e2024GC011656. https://doi.org/10.1029/2024GC011656.

Wang, X., He, K., Yang, C., et al., 2025. Formation mechanism of deep natural hydrogen in the Sichuan Basin. Sci. China Earth Sci. 68 (2), 581–597. https://doi.org/10.1007/s11430-024-1463-1.

Wang, G., 2023. Carbon dioxide capture, enhanced-oil recovery and storage technology and engineering practice in Jilin Oilfield, NE China. Petrol. Explor. Dev. 50 (1), 245–254. https://doi.org/10.1016/S1876-3804(22)60384-7.

Wei, R., Ma, H., Jin, Z., et al., 2023. New insights into the carbon cycle and depositional models of the Eocene saline lake, Jianghan Basin. China. Mar. Petrol. Geol. 149, 106079. https://doi.org/10.1016/j.marpetgeo.2022.106079.

Wu, H., Li, S., Wang, C., et al., 2024. Integrated chronostratigraphic framework for Cretaceous strata in the Songliao Basin. Earth Sci. Front. 31 (1), 431. https://doi.org/10.13745/j.esf.sf.2024.1.22.

Xie, H., Jiang, Z., Wang, L., et al., 2024. Organic matter enrichment model of fine-grained rocks in volcanic rift lacustrine basin: A case study of lower submember of second member of Lower Cretaceous Shahezi Formation in Lishu rift depression of Songliao Basin, NE China. Petrol. Explor. Dev. 51 (5), 1232–1246. https://doi.org/10.1016/S1876-3804(25)60537-4.

Yu, Y., Xu, Y., Xiao, Y., et al., 2013. The Controlling effect of source rock thermal evolution on hydrocarbon accumulation: In Dongling Area of Changling Depression, Songliao Basin. Nat. Gas Geosci. 24 (4), 712–718. https://doi.org/10.11764/j.issn.1672-1926.2013.04.712 (in Chinese).

Zhang, L., Zhang, X.J., Man, Y., et al., 2013. The analysis of sedimentary evolution mode of denglouku-formation in Gulong area of songliao Basin. Adv. Mater. Res. 652–654, 2501–2507. https://doi.org/10.4028/www.scientific.net/AMR.652-654.2501.

Zhang, M., Guo, Z., Sano, Y., et al., 2015. Stagnant subducted Pacific slab-derived CO_2 emissions: Insights into magma degassing at Changbaishan volcano, NE China. J. Asian Earth Sci. 106, 49–63. https://doi.org/10.1016/j.jseaes.2015.01.029.

Zhang, L., Li, X., Ren, B., et al., 2016. CO_2 storage potential and trapping mechanisms in the H-59 block of Jilin oilfield China. Int. J. Greenh. Gas Control 49, 267–280. https://doi.org/10.1016/j.ijggc.2016.03.013.

Zhang, Q., Timmerman, S., Stachel, T., et al., 2024a. Sublithospheric diamonds extend Paleoproterozoic record of cold deep subduction into the lower mantle. Earth Planet Sci. Lett. 634, 118675. https://doi.org/10.1016/j.epsl.2024.118675.

Zhang, S., Wang, H., Su, J., et al., 2024b. Control of Earth system evolution on the formation and enrichment of marine ultra-deep petroleum in China. Petrol. Explor. Dev. 51 (4), 870–885. https://doi.org/10.1016/S1876-3804(24)60512-4.

Zhao, X., Pu, X., Luo, Q., et al., 2025. Circle structure and orderly hydrocarbon accumulation of whole petroleum system in a continental fault basin: A case study of Kong-2 Member in Cangdong Sag, Bohai Bay Basin, China. Petrol. Explor. Dev. 52 (3), 1–11. https://doi.org/10.1016/S1876-3804(25)60590-8.

Zhou, S., Yu, B., Lintner, B.R., et al., 2023. Projected increase in global runoff dominated by land surface changes. Nat. Clim. Change 13 (5), 442–449. https://doi.org/10.1038/s41558-023-01659-8.

Zhu, R., Zhang, S., Wang, H., et al., 2024. Multi-spheric interactions driven differential formation and accumulation of hydrocarbon resources in the North Sea Basin. Sci. China Earth Sci. 67 (11), 3397–3420. https://doi.org/10.1007/s11430-024-1421-8.

Zhu, R., Zhang, W., Wang, H., et al., 2025. A theory of multi-spheric interaction-driven hydrocarbon formation and enrichment. Sci. China Earth Sci. 68 (8), 2492–2510. https://doi.org/10.1007/s11430-025-1617-y.